Composites Part C: Open Access 5 (2021) 100164

Contents lists available at ScienceDirect

Composites Part C: Open Access

journal homepage: www.elsevier.com/locate/jcomc

Cellulose nanocrystal based composites: A review

Jamileh Shojaeiarani [a], Dilpreet S Bajwa [b,*], Saptaparni Chanda [b]

[a] Department of Mechanical Engineering, Western New England University, Springfield, MA 01119, United States
[b] Department of Mechanical and Industrial Engineering, Montana State University, Bozeman, MT 59717, United States

ARTICLE INFO

Keywords:
Cellulose nanocrystals
characterization
Physico-mechanical properties
Processing
CNC Applications

ABSTRACT

Cellulose nanocrystals (CNC) have received much attention as renewable, biodegradable, nontoxic, and low-cost nanomaterials with some remarkable properties. Desirable engineering properties of CNC include large surface to volume ratio, high tensile strength (~10 GPa), high stiffness (~110–130 GPa), and high flexibility. They can be chemically modified to tailor their properties for high-end engineering and biomedical applications. Despite their outstanding properties, the wide-scale application is lacking due to their surface characteristics and processing challenges. To achieve their full potential safer extraction methods, improved surface modification and functionalization methods and processing techniques are being researched. This review attempts to access methods for characterizing CNC, and CNC composites as well as their emerging new applications as smart materials. The review is a valuable resource for researchers and scientists working in industry or academia to provide an update on the use of CNC materials and their composites in packaging, biomedical, and high-efficiency energy systems.

1. Introduction

Cellulose is an ageless biomaterial, found in abundance in the biosphere. For thousands of years it has been extensively used in weaving, pottery, textiles, cordages, clay bricks and as a fuel. Industrial applications of cellulose have evolved from construction material, paper, and textiles to modern cellophane films, dietary fibers, and advanced chemicals. However, in the last few decades' cellulosic research has exhibited a paradigm shift transitioning from macro, micro to nano scale. The explosive growth of nanotechnology has fueled rampant research on nanocellulosic materials. Cellulose nanomaterials are projected to be safe, sustainable, and less expensive with an impressive strength-to-weight ratio [1]. These characteristics have encouraged their use in new applications such as electronics, construction, packaging, food, energy, health care, automotive, and aerospace [2–4].

Nanocellulose market is expected to grow from USD 271.26 Million in 2017 to USD 1,076.43 Million by 2025 at a CAGR of 18.80% during this period [5]. The remarkable interest in nanocellulosic research can be gauged by the number of patents and publications in the last decade, roughly 100 patents per year [1,6]. National Nanotechnology Initiative (NNI) and EU Horizon programs have primarily funded the research activities US and Europe, respectively. In the US and Canada 15 companies are leading the nanocellulose production whereas Europe and Japan are projected as the largest market for nanocellulose [7]. Industrial collaborations such as GranBio Technologies with Birla Carbon, Borregaard participation with Bio-based Industries Consortium, and Imerys tie-up with leading papermakers have strengthened commercialization efforts [8].

The nanocellulose research is oriented around three forms, (1) cellulose nano-fibers (CNF) (2) cellulose nanocrystals (CNC), and (3) bacterial nanocellulose as shown in Fig. 1. Cellulose nanocrystals (less than 100 nm in one dimension) are widely exploited in the polymer composites as they are highly crystalline material with Young's modulus near 150 GPa and tensile strength 10 GPa. They exhibit surface charge, chiral nematic and amphiphilic properties, and serve to modify rheological, optical, and electrical properties of polymers. Nanocrystals have hydrophilic surfaces, but do not swell in water [9,10].

Despite their outstanding and diverse properties, wide-scale application of CNC is lacking in the commercial sector due to their polar and hydrophilic surface characteristics, and tendency to agglomerate in polymer matrices. Over the last few years, new surface modification techniques and mechanical processes have been introduced to address these problems. More recently several new commercial applications outside of paper and paperboard have been reported, including use of nanocellulose in oil and gas drilling fluids, adult diapers, coatings, composites, rubber latex, cosmetics, gel inks for pens, and foams for running shoes [1,11]. Biomedical market is exploring 3D printing of nanocellulose for tissue engineering, and wound dressing. In addition, spider-like network structures of CNF cryogel for air filters, and adsorbents for radioactive cesium ions [7]. Based on the growing interest in nanocellulosic materi-

* Corresponding author.
E-mail addresses: jamileh.shojaeiarani@wne.edu (J. Shojaeiarani), dilpreet.bajwa@montana.edu (D.S. Bajwa), saptaparni.chanda@montana.edu (S. Chanda).

https://doi.org/10.1016/j.jcomc.2021.100164
Received 6 December 2020; Received in revised form 25 May 2021; Accepted 26 May 2021

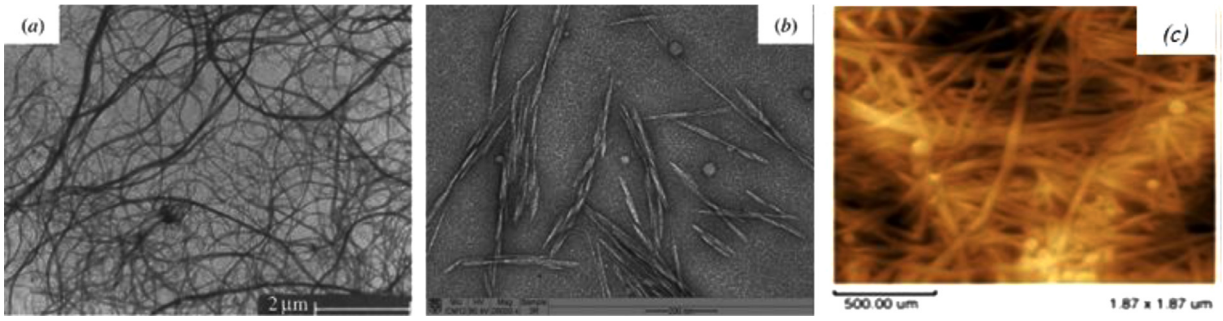

Fig. 1. Schematic of different types of nanocellulose (a) Transmission electron micrographs of cellulose nanofibers prepared from potato pulp (b) cellulose nanocrystals extracted from mengkuang leaf (c) Micrograph of bacterial cellulose(Reproduced with permission from [1,11]).

als, several review articles have been published describing their general characteristics, production methods and applications. However, there is very limited information available on the application of CNC in composites, processing technologies, and characteristics of nano-cellulose filled composites. With growing interest in CNC composites for high value applications in biomedical, packaging, electronics and energy there is a need for assessing current trends in research. This review addresses the current state of published knowledge on CNC characterization, processing of CNC based nanocomposites, characterization techniques, physical and mechanical properties, and emerging applications.

2. Isolation and pretreatment of cellulose nanocrystals (CNCs)

In the last few years, isolation and pretreatment of CNC from different sources and thereby revalorization of agro/ forest wastes has become center of interest to develop economic status of some countries. CNC can be isolated successfully from different agricultural sources- wood, cotton fiber, sisal fiber, bamboo residue. The agricultural wastes such as rice straw, rapeseed straw, corn stalks have gained special attention as novel sources of CNC. These agricultural wastes of shorter growing cycles can be disintegrated into CNC through delignification process, because of low lignin content.

Luzi et al. demonstrated a process to extract CNC from North African grass Ampelodesmos mauritanicus, commonly known as Diss. Before the extraction of nanocellulose, Diss stems were subjected to two different pretreatments (chemical or enzymatic). In case of chemical pretreatment, at the first stage sodium bi-sulphate (NaHSO4) was used to extract holocellulose (ȧ-cellulose+hemicellulose). Subsequently, sodium hydroxide (NaOH) was used to obtain ȧ-cellulose component and remove hemicellulose. In enzymatic pretreatment, xylanase and (Feedlyve AXC) and polygalacturonase (Peclyve EXG) enzymes were used. CNC was isolated from the pretreated material by sulfuric acid hydrolysis. Morphological investigation showed that both the pretreatments facilitated the reduction in fiber diameter. Analysis of X-ray diffraction spectra proved the formation of new crystalline domains resulted from the enzymatic degradation of cellulose. Chemically treated CNC showed lower diameter and length mean values as compared to the enzyme treated ones [12].

Yang et. al extracted CNC from Carex meyeriana Kunth via a combination of TEMPO oxidation and mechanical homogenization technique. The CMK fibers were treated with alkali-oxygen and PEG-salt ABS in to eliminate non-cellulosic substances. Then the degummed CMK was modified with dimethyl sulfoxide solution and subjected to a TEMPO oxidation and homogenization to extract CNC. The produced CNC showed an average diameter of about 33 ± 1.32 nm and length of 175 ± 3.21 nm. The crystal structure of CNC was not altered during the pretreatment processes, keeping the cellulose polymorphs intact. The extracted CNC exhibited much higher crystallinity than raw materials (CMK) and CMK fibers. While, the thermal stability of CNC was decreased [13]. Ferreira et al. obtained CNC from acid hydrolysis of bleached sugarcane bagasse pulp (SCB) and functionalized with adipic acid. SCB was subjected to a bleaching treatment using NaOH and H_2O_2. Then the bleached SCB pulp was hydrolyzed using sulphuric acid to extract CNC. The extracted CNC were surface modified by adipic acid. CNC extracted from bleached SCB exhibited hyphilic surface characteristic, relatively high crystallinity, and a high aspect ratio. The removal of amorphous regions resulted in a low nanocrystal dimensions in surface modified CNC. They also became less hydrophilic in nature.

Unmodified CNC can be used as reinforcing agents in hydrophilic polymer matrix, whereas modified CNC can be used for hydrophobic ones [14]. In an article of Abu-Danso, CNC were synthesized from absorbent cotton. Two pretreatments were done on the precursor (cotton) - dewaxing and bleaching with mild alkali. CNC were extracted via acid hydrolysis with sulfuric acid and a mixture of NaOH-thiourea-urea-H_2O helped in dissolution of cotton. There was a highly negative charge on the surface of cellulose and at pH 12, the extracted CNC showed higher negativity, over -30 mV. The CNC had high BET surface area, pore diameter and pore volume. The SEM images showed the flaky nature of the CNC. The pretreatments maintained the crystal structure of cellulose [15]. Kian et al. isolated CNC from roselle fiber derived from microcrystalline cellulose (MCC). In this study, acid hydrolysis with variable reaction times was conducted to degrade roselle derived from MCC to produce CNC. This method is proved to be cost saving as a yield of 21.92% CNC was obtained using a low chemical concentration of 50 wt% sulfuric acid solutions. The FTIR analysis indicated that the crystallites domains of CNC became increasingly compact with prolonged reaction time and no change in chemical structure. In TEM and AFM images, needle shaped CNC isolated from 45- to 60 min hydrolysis time were clearly visible. The isolated CNC had the highest crystallinity level of 79.5%, after 60 min hydrolysis. Furthermore, in colloidal suspension, CNC remained well dispersed, possibly facilitating nanocomposite fabrication. In thermal analysis though, all the CNC showed poor stability due to the surface sulfate component [16].

Li et al. extracted CNC from bleached chemical pulp via two stages of isolation techniques- Formic acid hydrolysis and TEMPO-mediated oxidation, under mild conditions. Formic acid was used in the first stage to eliminate hemicellulose and to release CNC by the swelling of cellulose fibers. Formic acid is readily recoverable and reusable. In the second stage, the isolated CNC were modified by TEMPO-mediated oxidation for modified surface properties. The modified CNC (T-CNC) had a length of 50-300 nm and a diameter of 2–4 nm, respectively. Higher carboxyl group content on the surface and more ordered crystalline structure helped T-CNC to disperse better and they showed higher viscosity in aqueous phase, compared to the unmodified [17]. Kunaver et al. developed a new production process of CNC from different cellulose containing natural materials. The process consisted of four steps- milling, glycolysis reaction, centrifugation and finally, rinsing with an organic solvent. CNC yield was between 56 and 75%. The liquification with glycols, using methane sulfonic acid as a catalyst was the key feature of this process to simplify the process of CNC production. During glycol-

ysis, lignin, hemicellulose, and other amorphous parts were liquefied leaving solid residue crystalline cellulose. Compared to the acid-based hydrolysis process, only 3% loading of acid was used. Four model materials were used in this method- cotton linters, spruce wood, eucalyptus wood and Chinese silver grass. The increased surface area of all the CNC reduced the thermal stability and this result completely matched with the crystallinity index [18].

Oun et. al isolated CNC from rice straw (RS), wheat straw (WS) and barley straw (BS) via acid hydrolysis method. The isolated CNC showed aspect ratio of 18, 16 and 19 with suspension yield of 64%, 75% and 69%, for the RS, WS and BS, respectively. The fibrous shaped CNC had length of 120–800 nm and width of 10–25 nm. The crystallinity index of CNC was increased due to the removal of amorphous region by sulfuric acid, and became 0.663, 0.710 and 0.634, respectively, for the RS, WS and BS. The thermal stability was also increased due to the removal of hemicellulose and lignin. These isolated CNC were used as reinforcement fillers to produce CMC/CNC composite films [19]. Dasan et al. developed a bionanocomposite of poly(lactic acid) (PLA) and poly(3-hydroxybutyrate-co-3-hydroxyvalerate) (PHBV) reinforced with CNC. The CNC was isolated via acid hydrolysis process from waste oil palm empty fruit brunch fiber. The resultant CNC was then functionalized by TEMPO-mediated oxidation and solvent exchange process. The fabricated composites with 0.25 wt% had shown improved interfacial adhesion, and thus enhanced mechanical, morphological and barrier properties. However, increased amount of CNC showed negative effects on composite properties because of agglomeration of CNC and reduced chain movement, respectively [20].

Jiang et al. isolated CNC from Humulus japonicus stem (HJS), a new low-cost source of cellulose material, via acid hydrolysis. The influence of the high temperature (HT) pretreatment on the properties of HT-HJS fibers and HT-CNC was studied. The average diameter and aspect ratio of CNC were 11.24 nm and 32.00, respectively. The initial degradation temperature was 212.8 °C and crystallinity was 70.05%. The HT-CNC had the same chemical structure as compared to the CNC. The average diameter of HT-CNC showed an obvious decrease and the aspect ratio showed significant increase, reaching a maximum value of 63.40. The HT-CNC displayed better thermal stability and crystallinity as compared to CNC [21]. Leão et al. evaluated the environmental and technical feasibility of CNC production from sugarcane bagasse fibers. Here, the life cycle assessment (LCA) was presented as a methodology to investigate the most feasible process. The processes V ($NaClO_2$/NaOH/H_2SO_4/30 min/1x) and IX ($NaClO_2$/NaOH/HNO_3/H_2SO_4/30 min/1x) showed the lowest environmental impact based on lowest water consumption and global warming potential. Furthermore, all processes showed that the pretreatment was the most important factor to the environmental impact increase. The effects of pretreatment conditions, for example bleaching (1x), hydrolysis time (30 min) and temperature (45 °C), were investigated on the morphological and thermal behaviors of the resultant CNC. The process IX proved to be the best, yielding CNC of 222 ± 23 nm length, and average diameter of 12 ± 1.6 nm. They exhibited low thermal stability (206 °C) and crystallinity index of 65% [22]. All natural sources of CNC and pretreatment processes are listed in Table 1.

There are other several examples of successful isolation of CNC from different natural sources, such as industrial waste cotton [23], garlic straw residues [24], barley straw and husk [25], eucalyptus pulp [26], oil palm frond biomass [27], onion skin [28], Calotropis procera biomass [29]. Acid hydrolysis, enzymatic degradation, or mechanical extraction such as high-pressure homogenization or ball milling were used to extract CNC from different sources. The extracted CNC were subjected to TEMPO-mediated oxidation, enzymatic, ultrasonication, high temperature or microwave-based pretreatment processes to improve their aspect ratio and crystallinity percentage. In most of the cases, the thermal stability and the tendency to agglomerate were decreased. All these aforesaid processes are successful to isolate CNC from different sources. Following the examples, there must be an elaborate research to find other natural or industrial waste resources and the most effective way to isolate CNC from them.

3. Characterization of cellulose nanocrystals

The properties and application of nanocomposites reinforced by CNC largely depend on different properties of CNC. Considering the potential applications and extensive commercial attention, great emphasis has been given to conducting a comprehensive study on structure and characteristics of CNC. To characterize the structure of CNC, the most important characteristics being studied are specific surface area, dimensions, shape, aspect ratio, crystalline structure, and charge. In this section the diverse examination techniques and specific features of CNC are described.

3.1. Turbidity

Turbidity is an optical characteristic of fluid and measures the amount of light scattered by suspected materials in the fluid when a light beam is passing through the sample. The principle of turbidimeter is based on the fact that when a light beam is passed through the suspension, some fraction of incident radiant energy is dissipated by absorption, reflection, and reaction whereas the residual is transmitted (Fig. 2). Turbidity graph of CNC is a simple and convenient measure of the flocculation potential of CNC in aqueous suspensions as an important behavior indicating the colloidal stability and nature of aggregates of CNC. The turbidity values and scattering of light depends mainly upon different factors related to physical characteristics of CNC such as shape, particle size distribution, refractive index, and the concentration of suspended CNC in the medium [30]. It also relates to the wavelength of light source employed in turbidity measurement. This test, however, is not applicable for aqueous suspension with high concentration of CNC and there is an upper limit of measurable turbidity. In fact, once the particulate concentration exceeds a specific level, the diffused light beam hits more suspended particles, multiple scattering happens, and absorption of light rises drastically. This in turn will result in a noticeable reduction in the path length of light beam in suspension which reduces the number of particles between the light source and detector and expands the upper point of turbidity [31].

To measure the stability of CNC suspensions, samples should be uniform, and degassed and repeated three times for reliable measurements. A comprehensive study conducted by Shimizu et al., evaluated the normalized turbidity values using AFM-derived thicknesses of CNC deposited on a flat mica surface [32]. In which, the turbidity of CNC dispersion as a function of mass–length ratio of CNC was described following Carr and Hermans method. They observed that light-scattering behavior and nanoparticle size measurement were slightly affected by interparticle interactions and higher values were reported for CNC thickness using turbidity test in comparison with AFM-measured thickness [32]. In a different approach, critical aggregation concentration of CNC in an aqueous suspension in presence of salt of various valences was evaluated considering the onset of turbidity in turbidity measurement. The onset of turbidity was nearly identical for different particle concentration including salts and CNC, confirming a balance of the attractive and repulsive forces in the system. However, at higher particulate concentration a strong concentration-dependence of colloidal stability and nature of CNC aggregates was reported [33]. In a similar study, the variation in turbidity values of CNC was reported and attributed to either sedimentation of aggregates or particles growth that follows classical theories in colloidal science [34]. Generally, the transmittance of aqueous CNC suspensions at 0.25–3.0 wt.% can be estimated at 500 nm and a typical transmittance value for a well dispersed 0.25 wt.% suspension is about 85%. The lower turbidity values specifies less aggregated CNC nanoparticles [35].

Although turbidity has been considered as a quick method to assess the width of various cellulose nanomaterials, due to the rod-like

Table 1
Sources of CNC and different pretreatment processes before CNC extraction.

Source of CNC	Pretreatment process	Ref.
Ampelodesmos mauritanicus fibers (Diss)	Dewaxing, treatment with 0.7% w/v solution of sodium chlorite ($NaClO_2$), 5% w/v solution of sodium bisulphate ($NaHSO_4$), 17.5% w/v solution of sodium hydroxide (NaOH)	[12]
Carex meyeriana Kunth	Heating in a mixture of 8 wt% H_2O_2, 1 wt% NaOH, 1 wt% JFC with a liquor ratio of 1:50, treatment with aqueous biphasic system containing 15 wt% PEG-2000, 4 wt% NaOH, 1.5 wt% Na_2SO_3, 1.5 wt% Na_2CO_3 with a liquor ratio of 1:20, blending with DMSO solution with a powder to liquor ratio of 1:30, TEMPO oxidation process	[13]
Sugar cane bagasse	Organosolv pretreatment using ethanol/water (1:1) v/v solution and a solid/liquid ratio of (1:10) w/v, bleaching treatment using NaOH (4%, 500 mL) and H_2O_2 (24%, 500 mL), sulfuric acid hydrolysis (65% v/v, 250 mL)	[14]
Medical absorbent cotton	Dewaxing in a Soxhlet extraction apparatus containing toluene and ethanol (2:1 v/v), bleaching using a solution of 0.1% sodium chlorite ($NaClO_2$)	[15]
Roselle fiber based MCC	Hydrolysis using 80 mL of sulfuric acid (50 wt%)	[16]
Bleached chemical pulp of birch (*Betula Pendula*)	Treatment using hydrochloric acid (varying from 0 to 3.17%, based on the total weight of the acid in the mixture), distillation using acetic acid, furfural and 5-hydroxymethyl furfural (HMF)	[17]
Cotton linters, Spruce wood, Chinese silver grass, Eucalyptus wood	Liquefaction of biomass using diethylene glycol, ethylene glycol, glycerin, mixtures of these alcohols (4:1 ratio), and methane sulfonic acid (3%)	[18]
Rice straw, wheat straw and barley straw	Filtration using a mixed solvent toluene and ethanol (2:1), bleaching using 1.4% w/v sodium chlorite and 5% acetic acid	[19]
Oil palm empty fruit brunch (OPEFB)	Alkali treatment using 100 mL of 2 M NaOH at 12.5% (w/v) loading- 80 °C, 120 min, bleaching operation using sodium hypochlorite (1.7 wt%) and in the presence of acetate buffer- ratio of fiber to liquor was 1:25 g/mL, 80 °C, 1 h, repeated 4 times	[20]
Humulus japonicus (HJS) stems	Treatment using ethanol ($W_{HJS}/V_{ethanol}$ = 1/20) for 14 h to remove wax and pectin, soaked in 4% w/v NaOH ($W_{HJS}/V_{4\%NaOH}$ =1/15 at 80 °C, 2 h to remove hemicellulose, 5% acidified sodium chlorite ($NaClO_2$+CH_3COOH, $W_{NaClO2}/W_{CH3COOH}$ = 1/1, W_{HJS}/V_{ASC} = 1/15, 80 °C, 6 h, 3 times, high temperature treatment – titanium alloy autoclave at different temperatures of 120 °C, 140 °C, 160 °C and 180 °C for 2 h	[21]
Sugarcane bagasse	Twelve different pretreatment conditions were followed using $NaOH/NaClO_2/H_2SO_4$ for 60 min	[22]
Industrial waste cotton	Treatment with hot water to remove wax and pectin, heated in hot air oven at 80 °C for 2 h, treated with 500 mL of 20% sodium hydroxide at 40-60 °C for 4 h to increase the crystallinity of cellulose, heated with 500 mL of 60% sulfuric acid at 50-60 °C for 8 h to remove hemicellulose and lignin	[23]
Garlic straw	Treatment with 2 wt% NaOH solution for 12 h to remove lignin and hemicellulose, bleaching using sodium chlorite solution at 80 °C for 2 h	[24]
Barley straw and husk	For barley straw: dewaxing using a mixture of toluene/ethanol (2:1 v/v) for 6 h, bleaching initially with sodium chlorite 0.7 (wt/v)% for 2 h, then using sodium hydroxide 17.5 (wt/v)% for 20 min For barley husk: Treatment with NaOH 4 (wt/v)% for 2 h at 100 °C under mechanical stirring, bleaching using a buffer solution of acetic acid, containing $NaClO_2$ 1.7 (wt/v)% under magnetic stirrer	[25]
Bleached soda-anthraquinone pulp of *eucalyptus* citriodora	Dissolved in 1% (w/w) ionic liquid 1-butyl-3-methylimidazolium chloride under microwave heating (150 °C, 400 W)	[26]
Oil palm fronds (OPF)	Treatment with a liquid containing 25% (w/w) soda concentration and 0.1% (w/w) anthraquinone to fiber ratio of 7:1 (v/w) at 160 °C for 120 min, bleaching using $MgSO_4$, NaOH, anthraquinone, H_2O_2 two times at 95 °C, 30 min, 80 psi pressure	[27]
Onion skin	Bleached with 0.7% (w/v) sodium chlorite solution (fiber to liquor ratio of 1:50) at pH 4 for 2 h to remove lignin, boiled with 250 mL of sodium sulfite solution for 5 h, treatment with 17.5% sodium hydroxide solution at 20 °C for 45 min	[28]
Calotropis procera fiber	Alkali treatment using NaOH solution (2 wt%), 100 mL, at room temperature for 3 h, delignification using acetic acid (93% v/v), 50 mL, and hydrochloride acid solution (0.3% v/v) under strong stirring for 3 h at 90 °C, bleaching using a mixture of H_2O_2 (5 wt%) and NaOH (3.8 wt%) at a ratio of 1:50 and stirred at room temperature for 3 h	[29]

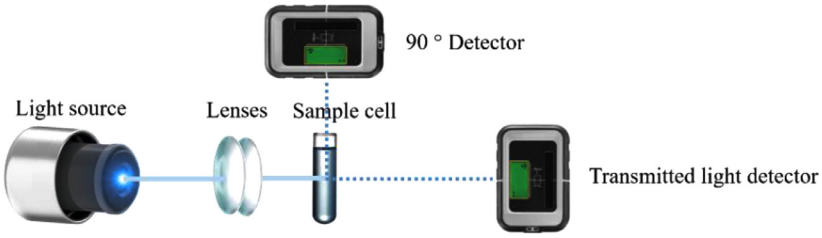

Fig. 2. Schematic representation of a general turbidimeter optical system.

or needle-shaped CNCs, the turbidity measurement mainly can provide information on fluctuation potential rather than particle size distribution. The other limitation of turbidity measurement is that the variations in turbidity can be attributed to several aspects mainly related to measurement process rather than nanoparticle aggregation. Therefore, to achieve reliable results turbidity should be combined with the other characterization methods such as Zeta potential.

3.2. Zeta potential

Zeta potential (ζ potential) is an analytical characterization technique to evaluate the surface charge of CNC in colloidal systems. The principle underlying the test is the electrochemical equilibrium at the particle-liquid interface. ζ potential measures the particle stability and charge repulsion/attraction between particles nearby the area restricted by the slipping plane and correspondingly is dependent on the location of slipping plane. Zeta potential measurement investigates the degree of electrostatic repulsion between neighboring, similarly, charged particles in a dispersion and provides broad insight into the dispersion, aggregation, or flocculation of nanoparticles such as CNC in colloidal system. Zeta potential depends heavily on the type of solvents, and the interaction between particles and solvent as the measured value is mainly an estimate of the gross charge of the suspension rather than the surface charge of an individual nanoparticle such as CNC. When ζ potential values for colloidal suspensions are either > +25 mV or < -25 mV, the particles are electrically stable [36]; on the other hand, the low value of ζ potential is an indication of poor state of dispersion and formation of aggregates due to low electrostatic repulsion forces between suspended particulates [37]. Typically, the ζ potential values for pristine CNCs are in the range of -20 – -50 mV (excluding CNCs extracted using HCl), while CNFs can have values near to -60 mV. Interestingly, as a suggestion to achieve an accurate ζ potential the fully dispersed 0.25 wt.% CNC suspensions or 0.05 wt.% CNF suspensions are required [38]. The addition of 5–10 mM salt such as NaCl has been also reported to improve the reliability of ζ potential measurement [39].

In addition to interaction between nanoparticles and solvent, in aqueous media, the pH of suspension is another important factor affecting zeta potential value. For a suspended particle with a negative value of ζ potential, the addition of alkali into system will increase the negative charge on particle. While the addition of acid will result in a positive charge if the ions are specifically adsorbed. In such an instance, a ζ potential versus pH curve will show positive values at low pH and lower or negative values at high pH. The point in which the ζ potential value is zero is known as isoelectric point. It is normally the point where attractive force between nanoparticles exceeds the repulsion and the colloidal system is least stable. In CNC extracted from sulfuric acid hydrolysis, the observed negative charge is due to the presence of sulfate ester groups (OSO_3^-). In a work, reported by Akhlaghi, et al. an increment in pH resulted in the segregation of the small amount of carboxylic acid groups on CNC, and this increased the value of the ζ potential mainly due to the increasing amount of negative charges (Fig. 3) [40].

Li et al., showed a strong relationship between ζ potential and pH for modified CNC, however, they claimed that ζ potential of pure CNC was almost identical across the whole range of pH [41]. At pH over 10, they observed a steep reduction in ζ potential due to the deprotonation

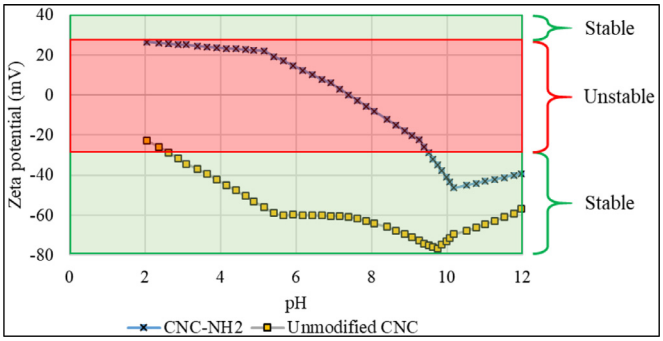

Fig. 3. Typical plot of zeta potential vs pH showing the stable and unstable region for suspended CNC (Reproduced with permission from [40]).

of functional group on the surface of modified CNC. The same results were reported by Prathapan et al., in which no substantial alteration was observed in the pH range of 2 – 10. However, at pH 1 a noticeable reduction in potential was observed owing to protonation of the sulfonic acids [42]. In a different work, ζ potential was employed to measure antifouling performance of graphene oxide-cellulose nanocrystal (GO-CNC)- PVDF composite membranes. Lv et al. reported higher ζ potential values for GO-CNC- PVDF was mainly due to the hydrogen bonds and intermolecular interactions between GO and CNC, which resulted in negatively charged oxygen-containing groups of GO-CNC [43].

Despite reports of zeta potential application in characterizing CNCs in a large number of papers, pH and temperature dependence results limit the accuracy of zeta potential in CNC suspensions with different temperature and pH. Furthermore, the results mainly assess the gross charge of the suspension rather than the surface charge of an individual nanoparticle such as CNC.

3.3. Transmission electron microscopy (TEM)

Transmission electron microscopy (TEM), an ultrasensitive method, has been widely applied to illustrate the structure, morphology, crystallographic and even chemical composition of an extensive variety of nanomaterials. In TEM process, the electron beam with the acceleration voltage in the range of 100–300 kV is transmitted through a specimen to obtain high spatial resolution. Electron density of material has a key role in contrast of TEM images and in cellulose-based materials such as CNC with high content of carbon, the electron density is low and this, in turn, will result in low contrast in TEM images [44]. Along with that, the average particle size of CNC (5 to 30 nm in diameter) is not big enough for transferring electrons to interrelate with the sample. Therefore, the low electron intensity and small thickness of individual CNC calls for the assistance of staining step prior to imaging to improve the contrast of TEM images. Nevertheless, problems regarding low contrast and blurry backgrounds will result in unreliable images with poor quality [45]. To address this problem, negative stain mainly composed of a heavy metal salt such as uranyl acetate [46] is applied to diluted CNC suspension and create an electron dense shield around CNC nanofillers. Thus, the individual CNC will be found as a clear item on a dark back-

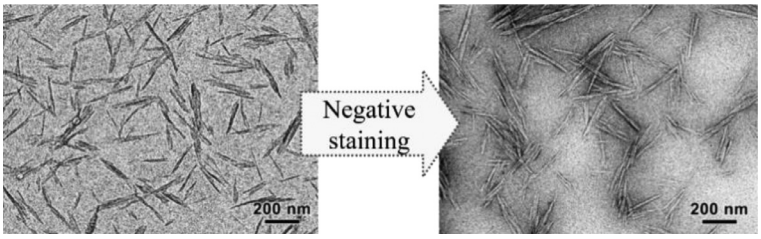

Fig. 4. TEM images of cotton-based CNC on glow discharged carbon-coated grid showing the effect of negative stain on the image quality. (Reproduced from Kaushik et al. with permission [50])

Table 2
TEM analysis conducted on CNC from different resources along with length and width of CNC measured by TEM.

Source	Volt. (kV)	Mag.	Size	Stain*	Grid	Glow discharge	Dispersion*	Contrast*	Ref.
Cotton	120	M	L=170 W=15	UA	Copper grid	Yes	G	G	[54]
Flax shives	80	O	L=2358 W=96	UA	Copper-coated formvar	Yes	G	G	[55]
Cotton	80	M	L=250 W=6	PA	Carbon-coated Copper	Yes	G	G	[56]
Biomass	120	O	-	UA	Copper	Yes	M	G	[57]
Cotton	-	O	L=145 W=4.76	PA	Plastic membrane coated	No	M	G	[58]
Sugarcane bagasse	-	O	L=133.8 W=96	PA	Copper	No	M	M	[59]
Seaweed	20	O	L=239 W=22.45	-	Carbon-coated copper	No	P	M	[60]
Pueraria root	80	O	L=330 W=60	PA	-	No	M	P	[61]

*Stain
UA: Uranyl acetate
PA: Phospho-tungstic acid

*Dispersion and Contrast
G: Good
M: Moderate
P: Poor

*Mag.
M: Acceptable magnification with extra contrast enhancement and staining (> 300 nm, < 1 μm scale)
O: optimal magnification range (< 300 nm scale)

ground. Moreover, the application of positively charged stain such as uranyl acetate [46] has been also reported as an alternative technique to improve the image contrast in TEM analysis. In some works, to increase the hydrophilicity of TEM grids and to improve the dispersion of CNC, glow discharge treatment has been used as an additional step prior to discharging CNC suspension on grid [47]. In this step grid surface is subjected to a plasma treatment, with different current values.

There are a wide variety of TEM grids for various applications and the right type of grid is required to obtain reliable images. The most commonly used grid for supporting CNC suspensions is copper grids [48,49], however, caution should be taken when the pH of the suspension is far low or high, as copper degradation might result in artifactual crystals or dendrites during drying [44]. In this regard, the application of carbon as an electron-transparent coating material for cupper grid not only provide an extra support for CNC suspensions but also limit the interaction between CNC and grid. Fig. 4 shows the TEM micrograph for cotton-based CNC on glow discharged carbon-coated grid before and after staining. The distribution of negative stain in TEM images suggest the more accurate estimation of CNC particle size.

In CNC characterization studies, TEM micrographs are mainly employed to estimate the morphology and particle size distribution of CNC nanoparticles. Many researchers have used ImageJ software to analyze the images and measure the dimension of individual CNC [51,52]. Table 2 summarize a list of TEM analysis conducted on CNC from different resources. The quality of TEM images (contrast and dispersion) is represented as a function of staining, discharging and accelerating voltage. As it was expected, glow discharge has an important impact on CNC dispersion on TEM images and staining process mainly improves the contrast of TEM images. However, the application of stain in TEM images might result in low resolution of TEM images, mainly due to the granularity of the dry stain. Therefore, a considerable amount of attention needs to be paid in staining TEM samples, and excess stain should be removed from sample to limit the possibility of formation of imperfectly stacked lamellar subunits around individual CNC [53].

In comparison with scanning electron microscope (SEM) and atomic force microscopy (AFM), TEM best suited for CNC characterization and can be employed to visualize the shape and structure of individual in the range of 100–200 nm. While AFM and SEM images normally show CNC aggregates in the form of clusters and individual crystals are not clear, due to high contrast in TEM images the individual crystals can be observed [44]. On the other hand, TEM allows crystallography diffraction experiment to visualize only two-dimensional distribution of CNC nanoparticles and for 3D analysis a combination of SEM and AFM is required.

3.4. Dynamic light scattering (DLS)

Dynamic light scattering (DLS), known as photon correlation spectroscopy (PCS) offers a complementary approach to nanoparticle size distribution in the colloidal suspension. In this technique, the hydrodynamic particle size of nanoparticles is measured using the time-dependent fluctuations of the scattered light at a specific scattering angle θ (right angle or back angle) (Fig. 5). The scattering angle is typically selected by the instrument maker regarding the inverse relation between particle size and scattering angle (173 ° for CNC) [62]. The DLS measurement is based on the fact that the dispersed nanoparticles such as

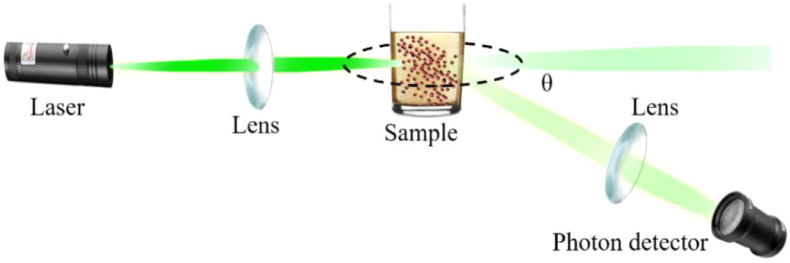

Fig. 5. Schematic diagram of an optical dynamic light scatter (DLS) used for particle size distribution measurement.

CNC in a suspension are undergoing Brownian motion, and the analysis of the intensity fluctuations over a short time yields the velocity of the Brownian motion of nanoparticles. This in turn can interpret the nanoparticle size using Stokes–Einstein equation [63]. Fixed angle and multi angle instrument are two types of DLS instrument, while multi angle instrument capable of measuring particle size distribution is the most common type of DLS used for CNC.

DLS analysis integrates any particle to spherical particles of equivalent volume, hence, CNC measurement is expressed as a hydrodynamic apparent particle size. Regarding the cylindrical structure of CNC and high aspect ratio, DLS should not be considered as the hydrodynamic radius and cannot be clearly related to the particle length or cross-section [64]. DLS measurement can be employed to detect the particle size distribution of CNC in a wide range of solvents, however, care must be taken in sample preparation as the colloidal stability over a time span which DLS measurements is conducted is vital for reliable results. For this purpose, the aqueous suspension is the most commonly system used for DLS analysis [65,66]. Although, DLS can provide facile measurement of the particle size of CNC, at typical concentration of CNC, results are distorted owing to particle-particle interactions. Therefore, the CNC suspension should be low enough (< 0.1 wt.%t) to form a clear suspension [67]. Besides particle size distribution, the formation of CNC aggregates, colloidal stability, and sedimentation kinetics have been also studied using the intensity profiles of DLS analysis. It has been reported that the size of CNC aggregates directly affects their velocity and smaller aggregates move faster than larger ones [68].

In addition to the failure of measuring the length of individual needle-shaped CNC, sample preparation and high concentration of CNC suspension is required for DSC measurement. In fact, in low concentration of CNC, multiple peaks and incorrect data may be found owing to the low scattering count.

4. Cellulose nanocomposites processing

The production of CNC nanocomposite has received increasing interest due to their promising mechanical characteristics combined with low density, biodegradability, and renewability. The incorporation of CNC into biodegradable polymers is even of more importance as it can result in not only an improvement in the performance characteristics of biopolymer, but also an accelerated biodegradation rate [69]. Cellulose nanocomposite study dating back to mid-90 s when Favier's research group incorporated monocrystals of cellulose with an aspect ratio around 100 into latex to advance the mechanical properties of latex nanocomposites [70]. Then after, extensive efforts have been conducted to prepare and characterize CNC nanocomposites using different techniques. In this section we describe several approaches to the preparation and characterization of CNC nanocomposites.

4.1. Cellulose nanocomposites preparation

One of the most important factors affecting the performance of CNC as reinforcing agent in different polymer matrices is the state of CNC dispersion and hence polymer matrix–CNC interaction. Beside the extensive research on the application of CNC in polymer matrices, achieving the homogeneous dispersion of CNC in polymer matrices, especially hydrophobic ones, is still the main challenge [71] in CNC nanocomposite manufacturing. The inherent hydrophilicity of CNC inhibits their proper homogeneous dispersion in non-polar [72] and hydrophobic [73] polymer matrices mainly due to van der Waals bonding. In this regard, the studies in the area of CNC nanocomposites are mainly inspired by the application of different techniques in improving the dispersion of CNC within polymer matrices. Although the research on surface modification treatments is beyond the scope of this article, it is worthy to note that the obvious effect of chemical treatment on reducing the hydrophilicity character of CNC have been extensively reported in the literature [74–77]. In this section, we highlight the mechanical techniques used for CNC nanocomposite manufacturing.

4.2. Solvent casting

Solvent casting or wet blending is a traditional thin film manufacturing technique with an optimal control on film thickness. In which, nanocomposite manufacturing starts with dissolving host polymer in a volatile solvent, followed by incorporating the nanofillers. After achieving a stable colloidal suspension of host polymer and nanofiller, nanocomposite film can be solidified into favored shape and geometry via solvent removal. Due to the hydrophilicity of CNC, water-soluble polymer matrices such as poly(ethyleneimine) provide the simplest systems for synthesizing CNC nanocomposites [78], while such nanocomposites have strength far below the potential strength of CNC. Thus, to achieve hydrophobic polymer nanocomposites reinforced by CNC, the major challenges are the improvement of adequate dispersion and high interfacial bonding between the polymer matrix and CNC. In this regard, to ensure the optimal dispersion of nanofiller within polymer solution and hence an improvement in interaction between polymer and nanofillers, wide range of chemical surface modification treatment have been extensively used to mitigate the hydrophilicity of CNC prior to suspension preparation. In addition to surface functionalization, ultrasonication treatment is another additional step in solvent casting manufacturing, facilitating the homogeneous dispersion of CNC within polymer matrix [79]. In which, acoustic energies delivered high power sonication and removes the van der Waals force between nanofillers [80], and thus permits the polymer chains to diffuse into open spaces among nanofillers.

The tedious solvent casting method with slow solvent evaporation rate favors the formation of CNC aggregates [81] and prevents the industrial exploitation of CNC nanocomposite. Moreover, the presence of residual solvent in solidified solvent cast film which results in a reduction in nanocomposite characteristics further limits the effective use of solvent casting technique in CNC nanocomposite manufacturing [82]. Therefore, along with ultra-sonication treatment, additional procedures such as air-forced drying [83], magnetic fields [84], electric fields [85], and surfactant [86] are also applied to CNC suspension to mitigate the negative aspect of slow drying rate in solvent casting method. Mechanical properties are critical for nanocomposite films and depend largely on the state of CNC dispersion within polymer matrix. Table 3 summarizes a short list of studies, in which solvent casting method has been employed to fabricate CNC nanocomposite and improved the mechan-

Table 3
Summary of CNC nanocomposites prepared by solvent casting method along with additional steps for strengthening corresponding composites.

Solution			Supplementary steps		Drying step			Film			Ref.
Host polymer	Solvent	CNC content	Modification	Sonication	Time	technique	Temp.	Thickness	E (MPa)	σ (MPa)	
	DMF	1.5	-	-	-	Pressure-	80°C	0.1 mm	15.4	9.4	[103]
polyurethane		5				Temperature			28.5	5.3	
		10				cycle			41.4	6.9	
		30							109	6.2	
PHB	DMF	2	-	Ultra-	12 h		80°C	40, 50 μm	2400	29.7	[104]
		4		sonication		Temperature			2500	29.2	
		6				cycle			2500	30.5	
SPEEK	Water-	1	-	Ultra-	24 h		60°C	70-80 μm	2522 2649	25.8	[105]
	ethanol	2		sonication		Temperature			2726 3447	34.78	
		3				cycle			3161	36.62	
		4								49.84	
		5								46.46	
PCL	THF	5	-	Solvent	Over night	Constant	25°C	-	200	10	[106]
		10		exchange		nitrogen			325	12.5	
		15				flow			460	15.5	
		20							500	16	
		25							640	17.5	
PBAT	chloroform	1	-	-	24 h	-	25°C	35 μm	2791	15	[107]
PVA	Water	1	Citric acid	Ultra-	24 h		40°C	-	1710	43	[108]
		3	modifica-	sonication		Temperature			1980	46	
		5	tion			cycle			2160	53	
		10							2360	46	
		15							2460	49	
PLA	Chloroform	1	Lauryl	-	24 h, 4 h	Pressure-	25°C and	50 μm	1740	45	[109]
		3	modifica-			temperature	50°C		1130	26	
		5	tion			cycle			1060	27	
		10							1010	21	
		20							950	18	

ical response of films in case of elastic modulus. The literature shows contradictory results concerning the effect of CNC content on mechanical properties of nanocomposite films, more likely due to the formation of CNC aggregates at high CNC contents.

4.3. Continuous melt extrusion

Melt extrusion or melt blending is a solvent-free procedure for plastic, rubber, and food industries, in which a product of uniform shape and density is formed through a combination of heat, pressure, and friction. Melt extrusion dates to the early 1930s [87] and soon after, it has become one of the most widely adopted manufacturing techniques in polymer-based nanocomposites of thermoplastics or elastomeric polymers. Among different melt extruder, the screw extruders are the most common type in polymer industry as they continuously convert polymer pellets into finished form such as filament or extrudates. CNC nanocomposite melt extrusion can be performed using twin [88] or single [89] screw extruder with various modular screw configurations. Twin-screw extruders can be either, co-rotating or counter-rotating depending upon the screw configuration. In nanocomposite manufacturing, co-rotating twin-screw extruders are more preferred than single screw due to the effective nanoparticles dispersing configurations [90]. Twin screw extruders are often used to process highly viscous materials and remove large extents of volatile substances, while simple screw extruders have better performance in mixing materials [91].

Despite the extensive use of melt extrusion in composite manufacturing, surface charge density, poor compatibility between CNC and polymers [92], and mechanical and thermal degradation of CNC at elevated temperatures [93] impose restrictions on effective melt-compounding of CNC within hydrophobic polymer. To tackle these issues, different approaches have been proposed in the literature. In order to lower the surface charge density, hydrochloric acid (HCl) and phosphoric acid (H_3PO_4) have been used alternatively in acid hydrolysis of cellulose [94]. Spray freeze-drying technique has been also recognized as an effective method for drying cellulose nanomaterials and limiting the formation of irreversible and hard packed aggregation of CNC which can be obtained during typical spray drying or freeze-drying techniques [95]. The concepts of physical coating [96] and surface modification treatment of CNC [97] are another suggestions to provide a high level of protection against thermal degradation. However, an extra caution should be taken since additional materials can influence the overall characteristics of final product.

In some cases, to further enhance the uniform dispersion of CNC through polymer matrix, the concept of two-step dispersion processes based on highly concentrated masterbatch as a source of CNC has been reported. In this technique, high CNC content masterbatch in form of thin film [98], freeze-dried suspension [99] or pellet [92] are used to incorporate CNC to the host polymer in a stepwise fashion (Fig. 6). The CNC masterbatch is diluted by the addition of host polymer in melt extrusion process with the goal of achieving an optimal dispersion. Reid research group [38] using masterbatch approach, prepared PEO-CNC nanocomposite and found a significant improvement in CNC dispersion and thermal characteristics in comparison with direct addition of CNC. In a similar work, CNC was incorporated into PLA matrix using high content masterbatch followed by melt mixing not only to improve the CNC dispersion, but also to enhance the mechanical properties of host polymer. They showed that the application of solvent casting before extrusion resulted in the relatively good dispersion and hence a significantly larger amount of interfaces between nanofillers and polymer matrix that can then overwhelm the basic nanoparticle effect and lead to higher stiffness for CNC nanocomposites [100].

Direct liquid feeding of aqueous CNC suspension is another approach in nanocomposite manufacturing to mitigate the risk of CNC aggregates in polymer matrix. In liquid feeding, an aqueous suspension of CNC is pumping to the extruder during compounding, while the miscibility of the aqueous medium and host polymer should be carefully certified otherwise, phase separation might happen in final product [101]. Temperature profile in melt extrusion is mainly adjusted considering glass transition, melting point, and rheology of host polymer than CNC thermal stability. Therefore, thermal degradation and discoloration have been occurred for CNC-containing nanocomposites. To lower the risk of CNC

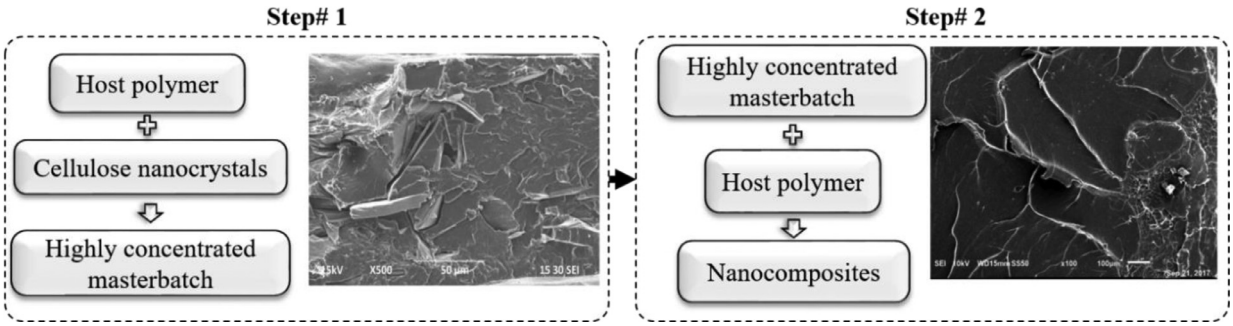

Fig. 6. Schematic diagram of 2-step dispersion process of melt extrusion in masterbatch concern. (Reproduced with permission from [98]).

thermal degradation in polyamide 6-CNC water assisted compounding extrusion process, Peng et al. pumped CNC suspensions into the middle zone of a twin-screw extruder while lowering the processing temperatures by 30 °C [102]. The granulated compound achieved after evaporating water at the last metering zone was then molded in an injection molding machine. Although the agglomeration of CNC in nanocomposite samples was mitigated, an additional molecular weight of host polymer was observed due to thermal and hydrolytic degradation during nanocomposite processing.

4.4. Batch processing

Batch mixing process is a sequential process, convenient for small scale nanocomposite preparation. This method has been extensively used in academic researches focused on characterization of small batch of CNC nanocomposites [110,111]. Typical batch mixers are composed of counter-rotating roller blades in a twin-cylinder configuration capable of melting and mixing polymers. The capacity of splittable barrel might be either 5 or 15 ml depending on the batch size and extended fully intermeshing conical screws are designed by manufacturer with fixed geometry. The main limitation of this method in CNC nanocomposite manufacturing is long processing time, which can result in thermal degradation during the residence time and hence decoloring of final product [111]. Furthermore, the shear forces provided in a batch mixer is insufficient to prevent the formation of agglomeration of fibers during nanocomposite manufacturing [112]. In a competitive study by Bagheriasl, internal batch mixer and extruder were employed separately to evaluate the performance characteristics of PLA-CNC nanocomposites via the application of masterbatch or direct mixing of PLA-CNC. They observed significantly higher complex viscosity and storage modulus in PLA-CNC nanocomposite prepared via a twin-screw extruder than internal batch mixer samples. They attributed such a noticeable discrepancy to the formation of an interconnected structure of CNC in PLA matrix due to well dispersed CNC in PLA-CNC nanocomposites prepared via masterbatch approach and twin-screw extruder [113].

In another attempt for preparing composites samples using bath mixing with a residence time of 8-10 min at 232°C, the addition of CNC into polyamide 6 lowered the impact strength of composite in comparison with pure polymer matrix, owing to poor dispersion quality of CNC in polymer matrix. Long residence time and high temperature in batch processing also resulted in thermal degradation and color change in PA6-CNC samples (Fig. 7) [114], however, in a different attempt it was reported that the discoloration is not linked to the mechanical behavior of CNC nanocomposites. As the discoloration is not ideal mainly for nanocomposites with optical application, to mitigate the risk of thermal degradation during long residence time in batch mixer several researchers used thermal stabilizer during processing stages [115].

Wet ball-milling is another nanocomposite manufacturing technique aiming on good temperature control during CNC nanocomposite manufacturing. Kedzior et al. employed wet ball-milling for the first time to prepare PMMA-CNC nanocomposite. In this study, CNC and PMMA-grafted CNC solution was added into PMMAin plastic Nalgene bottle containing methyl ethyl ketone and stainless-steel milling media (0.8 mm diameter beads). The processing was conducted at 175 rpm for 24 h, and to remove milling media and vaporizing methyl ethyl ketone, the mixture was filtered and stored under hood. The solid composites were then broken and hot-pressed at 160° C. Although, nanocomposite samples exhibited low variation in color due to low exposure to high temperature, foam structure was observed for ball-milled samples owing to methyl ethyl ketone evaporation, (30 s^{-2}. min). In addition, the presence of solvent in wet ball-milled samples and the effect of vaporizing methyl ethyl ketone of the nanocomposites during hot pressing lowered the Young's modulus of wet ball-milled samples [116].

5. Cellulose nanocomposite characterization

5.1. Morphology

Pristine CNC and surface modified CNC, both affect the morphology of the composites in some manners. In case of pristine CNC, there is more agglomeration in the matrix which in turn affect the overall mechanical properties of the composites. But in case of surface modified CNC, the dispersion of nanoparticles is improved enhancing the mechanical properties of the composites, keeping the original nanostructured morphology intact. For this reason, it is very important to study the change in morphology of CNC incorporated polymer composites to understand its effect on the overall properties of the composite. Zhang et. al grafted Poly (methyl methacrylate) (PMMA) and poly (butyl acrylate) (PBA) onto CNC and produced modified CNC (MCNC). They prepared a microphase separated MCNC/ PBA-co-PMMA nanocomposite and studied its morphology. The rod-like morphology was clearly observed in TEM for the pristine CNC, having the mean diameter and length of 18 and 213 nm, respectively. In case of the grafted CNC, the rod-like morphology was well-preserved even after the grafting polymerization, having the length and width of 250 and 25 nm, respectively. The fractured surfaces of the nanocomposites showed bi-continuous ductile fractured morphology and the irregular fractured surfaces of the CNC was clearly observed. This indicated that improved chain entanglement and hydrogen bonding interactions facilitated improved compatibility between the MCNC and the polymer matrix [117].

Arrieta et al. synthesized CNC from microcrystalline cellulose via acid hydrolysis and incorporated them into poly (lactic acid)-poly (hydroxybutyrate) (PLA-PHB) blends to enhance the overall properties of the multifunctional system. TEM images of the pristine CNC and surfactant modified CNC (CNC) showed length of 100–300 nm and width of 5–10 nm. Morphological features of the cross cryo-fractured sections of pure PLA, PLA-PHB blend, binary and ternary nanocomposites were inspected using FESEM. A typical smooth and uniform surface was exhibited by pure PLA films, while the PLA-PHB blend exhibited a tougher surface due to increase in crystallinity. The pristine CNC incorporated nanocomposites showed poor interfacial adhesion, but the surface modified ones showed better dispersion indicating enhanced interfacial ad-

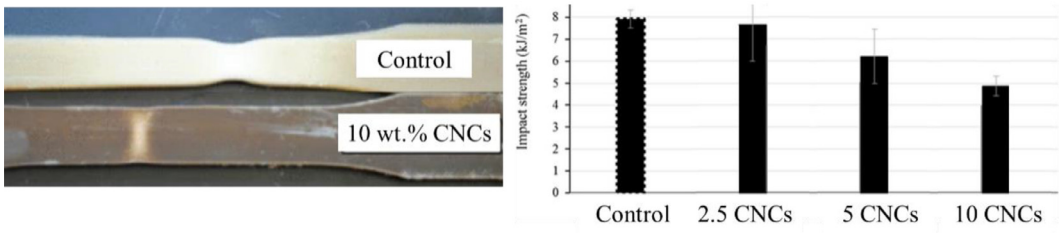

Fig. 7. Color change in the composite sample due to thermal degradation and the impact strength of PA6-CNC composites at different CNC loadings (2.5%, 5%, and 10%) (Reproduced with permission from [114]).

hesion and increased compatibility between matrix and nanoparticles. An AFM analysis was also done to study the nanocrystal dispersion. The pristine CNC incorporated films appeared agglomerated, but the CNC incorporated films showed more individualized structure. This confirmed the effect of surfactant on the surface of the CNC allowing the polymer chains to penetrate between the cellulose structures [118]. Li et al. constructed nanocomposites composed of poly (butylene succinate) (PBS) and CNC by solution coagulation method. The morphology of the PBS/CNC nanocomposites was studied by SEM. A smooth surface was exhibited by neat PBS, and the rough surface by PBS/CNC films, roughness increasing with the increase in CNC loading. No aggregation of CNC was detected when the loading was increased up to 1 wt%. A good interfacial adhesion between the matrix and CNC was detected as there was no pulling out of CNC. Therefore, when external force was applied, CNC broke causing deformation in the surrounding matrices which increased with increased content of CNC in composite [119]. Zarina et al. produced CNC from kenaf fibers and incorporated them as reinforcing agents in biocomposites based on κ-carrageenan. The carrageenan composite film with 4% CNC content exhibited high level of dispersion and distribution of CNC within the polymeric matrix. The structural similarity between the matrix and CNC facilitated the hydrogen bonds between hydroxyl groups and thereby the compatibility between the nanofillers and the matrix. However, when the CNC loading reached 8%, the fillers tended to agglomerate due to self-association via hydrogen bonding. Agglomeration of CNC reduced the filler-matrix interfacial contact, resulting in poor interfacial stress transfer [120]. Mi et al. produced poly (ε-caprolactone) (PCL)/ CNC nanocomposites via twin-screw extrusion. The injection molded samples were fractured in cross-section to study the dispersion of CNC in polymer matrix. CNC were detected as small dots and were dispersed uniformly in the matrix. The alignment of CNC was induced by the melt flow direction. More bumps like ridges were detected with the increase in CNC content, indicating CNC in other directions were buried in the polymer matrix. The 5% CNC loaded samples indicated aggregation of CNC in the PCL matrix. There was no clear void observed in the images, confirming the strong interfacial bond between the matrix and the nanofillers, as the CNC were broken instead of being pulled out of the polymer matrix [121].

There is an improvement in adhesion and interfacial bonding between the polymer matrix and nanofillers due to the incorporation of surface modified CNC in the composite system. The overall stress transfer was also enhanced, but up to a certain extent. Along with CNC loading, the agglomeration of nanofillers was also increased. There several other researches [111,122,123] were the morphology of the CNC incorporated composites was discussed. There is a huge scope of further research to improve the dispersion of CNC in polymer matrix.

5.2. Thermal properties

Surface modification of CNC sometimes can substantially affect the thermal characteristics of native CNC. Generally, functional groups are attached to the CNC surface via surface modification. These functional groups can change the thermal stability and crystallization behavior of native CNC due to chemical reactions. As a result, when these modified CNC are used as reinforcement for composites, the overall thermal properties of composites are also changed. Tanpichai et. al fabricated a CNC reinforced poly (vinyl alcohol) (PVA) hydrogel with high water content (~92%), using glutaraldehyde (GA) crosslinker. The change in thermal properties due to the addition of CNC in the cross-linked hydrogel was investigated. The CNC used in this research contained surface sulfate groups, because of which the CNC showed significantly lower thermal stability. Therefore, the onset degradation temperature was decreased due to the incorporation of the CNC in hydrogels. When the CNC content was increased, the onset degradation temperature was significantly reduced from ~347 °C for cross-linked PVA to ~320 °C for cross-linked PVA2.0 (CNC content). The lower thermal stability of CNC might be the cause of this reduction [124]. Kargarzadeh et al. produced a new nanocomposite of an unsaturated polyester resin (UPR) and CNC. Here, the CNC were silane treated and the effect of silane treatment on the thermal properties of CNC were studied. The nanocomposites incorporated with native CNC (2 and 4 wt%) showed an initial weight loss at ~140 °C. at ~370 °C, there was a decomposition attributed to CNC and the main decomposition was at ~380 °C due to UPR. But in case of the nanocomposites prepared with silane treated CNC (STCNC), the onset degradation temperature is much lower as compared to the native ones. However, the main decomposition was observed at ~388 °C. The thermal stability improvement of CNC was caused by the strong filler-matrix interaction, especially after the silane treatment. There was a chemical bond formation between the CNC and the matrix, provided by the silane coupling agent [125].

Spinella et. al prepared a nanocomposite with acetate and lactate modified CNC (AA- and LA-CNC) and polylactide (PLA), to improve the heat deflection temperature of PLA. The thermal stability of the CNC prepared by the modified Fischer esterification method was investigated by Thermogravimetric analysis (TGA). LA-CNC exhibited the highest thermal stability followed by the AA-CNC. The derivative thermogravimetric curve (DTG) revealed that the stability of LA-CNC is about 40 °C higher than the acid derived CNC. All the nanocomposites showed a reducing trend of thermal stability, acid derived ones (HCl-CNC) exhibiting the lowest. AA- and LA-CNC contained composites showed less pronounced decrease in thermal stability. The weak adhesion and therefore the poor dispersion of the acid derived CNC in matrix, may be the cause of the reduced thermal stability. In case of AA- and LA-CNC, the dispersion of CNC may be relatively better [126]. Dhar et al. reported a reactive extrusion process using only a single step, to produce the polylactic acid grafted cellulose nanocrystals composite films (PLA-g-CNC) of improved thermal stability. As usual, neat PLA exhibited a one-step degradation behavior, with a onset temperature of ~306 °C and T1/2 (50% reduction of weight) of 356 °C. These degradations reportedly caused by hydrolysis and oxidative chain scission. However, the reactive extrusion approach to graft CNC onto PLA using a sparse amount of crosslinking agent helped to significantly improve the thermal stability of PLA. Both Tonset and T1/2 were increased by ~12 °C and ~5 °C, respectively, than neat PLA. During the reactive extrusion process, the formation of PLA encapsulated CNC successfully masked the sulfate and hydroxyl groups of CNC, causing delayed degradation. Also, higher activation energy was required to break the preformed C-C bond be-

tween the PLA and CNC, thereby leading to enhanced thermal stability [127].

Zhang et al. modified pristine CNC surface properties by grafting poly (methyl methacrylate) (PMMA) and poly (butyl acrylate) (PBA) onto CNC surface. The thermal degradation properties of the pristine and grafted CNC were compared by TGA analysis. It was evident from the TGA data, that the hydrophobic coating of PMMA and PBA caused less thermal degradation at lower temperatures as compared to the pristine ones. Additionally, the major degradation step occurred at higher temperature, due to the masking of surface sulfate groups of CNC by the grafted copolymers. The hydrophobic coating of polymers reduced the water adsorption capacities from hydroxyl groups present in CNC surface, thereby stabilizing CNC during decomposition. Modified CNC produced less amount of char than the pristine ones [117]. Arrieta et al. added CNC in poly(lactic acid)-poly(hydroxybutyrate) (PLA-PHB) blends to enhance the structural and thermal properties of the composite systems. In this case, a surfactant modified CNC (CNCs) was used to improve the interfacial adhesion while retaining the thermal stability. Both CNC and CNCs were observed to improve the thermal stability of PLA-CNC and PLA-CNCs blends. But in terms of weight loss, the addition of the nanocrystals to the PLA-PHB blend showed decreased thermal stability as compared to the neat blend. However, slightly better thermal stability was observed when CNCs was added to the blend system. In case of PLA-CNC (binary nanocomposite) blend, the degradation process was shifted to lower temperature. But under 200 °C, no degradation occurred, indicating better thermal stability. The onset of degradation process was shifted to the higher temperature due to the incorporation of CNC and CNCs to the PLA-PHB blend, indicating enhanced thermal stability of ternary nanocomposites [118].

There are several other examples [128–130] of change in thermal stability of composite systems due to the incorporation of CNC. In most of the cases, surface modified CNC showed better performance in terms of enhancing the thermal stability of the composites. The better dispersion of CNC caused by surface modification led to better interfacial adhesion to the matrix and thereby the increase in thermal stability of the entire system. Following these examples, an elaborated research must be conducted to investigate the effect of CNC incorporation on the thermal stability of a composite system.

5.3. Rheological characteristics

Surface modification of CNC attached functional groups to CNC surface to avoid agglomeration of CNC during composite manufacturing. The rheological responses of the CNC filled polymer melt are dependent on the degree of dispersion of CNC particles, their orientation state and aspect ratio. Due to this reason, the rheological properties of the melt were also affected and the comparatively homogeneous dispersion of CNC led to the effective load transfer to the reinforcements. Pinheiro et. al studied the effect of incorporation of octadecyl isocyanate modified CNC on the rheological properties of the nanocomposites of poly (butylene adipate-co-terephthalate) (PBAT) matrix. The unmodified CNC induced PBAT nanocomposite showed visual agglomeration of CNCs. Modified CNC-based (MCNC) based PBAT nanocomposite showed a shift in both storage and loss modulus as compared to the neat PBAT samples, which showed a declining trend as the CNC content increased. More homogeneous dispersion of nanoparticles led to improved load transfer when the MCNC loading was increased up to 3 wt%. However, when the concentration of MCNC was increased from 3 wt%, that led to the formation of non-homogeneous domains and eventually affecting the viscoelastic properties of the composites. The complex viscosity (η^*) was also measured and it showed a decreasing trend when the concentration of MCNC was increased from 3 wt%. This phenomenon may be attributed to the increased agglomeration of nanoparticles and reduction of the free volume of the nanocomposites [131]. Wang et al. incorporated pristine and acetylated CNC with poly (ε-caprolactone) and performed an elaborate study with various flow fields, including linear and non-linear dynamic shear flow, creep and start-up flow. The improved phase affinity of the acetylated CNC yielded diluent effect, thereby exhibiting higher percolation threshold than the pristine ones. The formation and building of the percolated network were facilitated by the Brownian motion of the particles. Brownian motion is nearly independent of the altered phase affinity. Moreover, these kind of interactions played a dominant role to determine the overall creep strain levels of the nanocomposites [132].

Zhang et al., uniformly dispersed the CNC in the poly (lactic acid) (PLA) matrix via the Pickering emulsion approach. The increase in storage modulus compared to the neat PLA melt was showed by the CNC incorporated nanocomposites and also formed a plateau at lower frequency regions. A long plateau region in the complex viscosity (η^*) curve of neat PLA sample was observed, while at higher frequencies there was a slight shear-thinning behavior. Good dispersion of CNC in the PLA matrix promoted the formation of network and transition from fluid to solid at higher temperatures, indicated by the shear-thinning behavior of all composites without any plateau region, at lower frequencies [133]. Gupta et al. used spray-dried and lignin coated CNC (L-CNC) to improve the rheological properties of the poly(lactic acid) (PLA) composites. Both the complex viscosity and storage and loss moduli of the polymer melt were increased due to the presence of L-CNC. The melt viscosity and storage modulus at the region of low frequency were dramatically improved at 0.7 wt% of L-CNC, gradually converting from a liquid to solid and thus indicated a network structure formation. The rheological percolation threshold concentration of PLA/L-CNC nanocomposite was found to be 0.66 wt%, significantly lower than the other previously reported values of PLA/CNC composites. The significantly low percolation threshold concentration was the result of the uniform dispersion of L-CNC in the PLA matrix and the increased compatibility between the lignin and the polymer [134]. Shojaeiarani et al. studied the influence of masterbatch preparation techniques on the rheological properties of poly(lactic acid) (PLA)-CNC composites. In this article, film casting and spin coating were used to prepare masterbatches. The CNC were modified using poly(ethylene oxide) (PEO) and incorporation of these p-CNC into PLA exhibited enhanced storage modulus, as the p-CNC acted as reinforcement agent for the composites. The spin-coated samples having higher molecular weight showed higher storage modulus than their film casted counterparts. However, in case of spin-coated composites tan δ curves exhibited higher peak value because of their higher dispersity index. Both the PLA and nanocomposites indicated a non-Newtonian behavior in case of their complex viscosity at low shear rates, and subsequently a shear thinning behavior. The spin-coated composites showed higher complex viscosity and shear thinning behavior than the film casted ones, because of their higher molecular weight [135].

There are several other studies [136–139] on the effect of incorporation of CNC in polymer nanocomposites. The rheological properties of different CNC based composites are listed below in Table 4. In most of the cases, the storage modulus and complex viscosity were increased due to the presence of CNC in the nanocomposites. Also, the rheological percolation threshold concentration was decreased in presence of surface modified CNC. These phenomena may be attributed to the improvement in dispersion and distribution of CNC in the polymer matrix and also good compatibility between CNC and polymer. Following these examples, further research must be conducted in future to investigate the effect of CNC incorporation on the rheological properties of different polymer composite system.

5.4. Barrier properties

Global environmental awareness in replacing traditional polymers by biodegradable packaging materials has been interested scientists and industries in presenting new natural polymers. Despite great developments in biopolymers, the application of natural polymers for food packaging still suffers from poor barrier performance against oxygen, water

Table 4
Summary of the rheological properties of different CNC based composites.

Composition		Rheological properties			Ref.
Host polymer	CNC content	Storage modulus (GPa)	T_g (°C)	Tan δ	
PCL	1 wt%	11.65	-	-	[180]
	3 wt%	21.11	-	-	
	5 wt%	32.28	-	-	
	Acetylated 1 wt%	25.92	-	-	
	3 wt%	35.32	-	-	
	5 wt%	42.75	-	-	
PBST70	0 wt%	3.44	-11.7	-	[187]
	1 wt%	3.69	-11.8	-	
	3 wt%	4.02	-11.8	-	
	5 wt%	4.67	-11.1	-	
PBST50	0 wt%	3.39	-9.4	-	
	1 wt%	3.53	-8.8	-	
	3 wt%	3.84	-8.5	-	
	5 wt%	4.33	-8.2	-	
PBST30	0 wt%	3.40	7.8	-	
	1 wt%	3.98	8.3	-	
	3 wt%	5.53	9.6	-	
	5 wt%	6.35	9.8	-	
PLA	0 wt%	2.00±4.0	65.16±1.5	2.72±0.02	[183]
PLA	1 wt%	2.50±5.2	65.92±1.6	1.83±0.06	
(Film casted)	3 wt%	2.39±6.3	67.8±1.2	2.65±0.01	
	5 wt%	2.30±10.7	65.99±2.0	1.78±0.03	
PLA	1 wt%	2.84±6.1	65.18±1.3	2.23±0.04	
(Spin coated)	3 wt%	2.46±2.6	67.05±0.8	2.57±0.03	
	5 wt%	2.05±3.5	65.71±1.2	1.96±0.04	

vapor and light. In this regard, incorporation of nanosized fillers such as CNC into natural polymers is considered as a possible solution. Promising mechanical properties, highly crystalline structure, worldwide availability, biocompatibility, and biodegradability, make CNC as a promising bio-based material in food packaging industry. In the literature, it was reported that the addition of CNC improved the general barrier characteristics required for food packaging via reducing water vapor and oxygen permeability in polymer films mainly due to high crystallinity [140,141].

The great interest in the application of CNC as barrier improver in packaging nanocomposite is due to the fact that the presence of high aspect ratio CNC in polymer matrices could provide large surface areas with promising reinforcing effects [142]. Furthermore, the presence of high aspect ratio CNC in the packaging materials can drop the transfer rate of different molecules such as oxygen, carbon dioxide, and water vapor crossing the package via increased tortuosity of the diffusive path for permeants.

In particular, the use of CNC as biobased nanofillers has been widely studied to improve the barrier properties of PLA. For instance, Fortunati et al, conducted a study on the application of modified and pristine CNC on barrier properties and migration behavior of PLA-based nanocomposites. They reported that surfactant modified CNC dispersed uniformly in PLA and significantly reduced the water permeability. They also observed little tortuosity in PLA nanocomposites due to the incorporation of CNC [185]. In another research, the combination of surfactant modified CNC with silver particles in improving the barrier properties of PLA was reported. In addition to higher barrier properties, the addition of silver particles and CNC resulted in antimicrobial activity in nano-biocomposite films. However due to lack of enough information on health effect of silver nanoparticles, its application can commercialize at this time [143].

According to the results of Lengowski, the oxygen transmission rate (OTR) required for most food products should lie below 10–20 $ml.m^{-2}day^{-1}$ [144], while from a report by Chen et al. OTR for CNC reported as 0.6 ml.μm/m2.day.kPa [145]. Therefore, employment of CNC as a modifier for OTR in form of film, coating, or filler materials can increase the oxygen barrier properties of packaging materials. In this regard, Azizi et al. reported OTR for the poly(vinyl alcohol)/chitosan bionanocomposite films with thickness of 0.2 mm as 35.9 $ml.m^{-2}.day^{-1}$. While the addition of CNC as nanofiller significantly decrease OTR to as low as 12.4 $ml.m^{-2}.day^{-1}$ in nanocomposite films reinforced by 3 wt.% CNC [146]. In another study, coating PLA film with CNC resulted in a noticeable improvements in oxygen barrier properties of film and decreased it from 18.65 (ml.μm)/(m^2.day.kPa) for PLA film to 0.029 (ml.μm)/(m^2.day.kPa) for CNC coated PLA film [147].

Water vapor permeability (WVP) also known as water vapor transmission rate (WVTR) or moisture vapor transmission rate (MVTR) is a measure of the passage of water vapor through packaging materials represented as the water mass per unit area, per unit time. For an efficient preservation of packed food, the water vapor barrier properties need to be considered as an important factor specially for food items which are susceptible to moisture content equilibrium. The semipermeable nature of the polymer films permits a high rate of water vapor transmission through the film, hastening food spoilage as a result of the existence of moisture. The WVP of packaging materials mainly govern by film purity, hydrophilic–hydrophobic ratio [148], crystalline and amorphous ratio [149], and the polymer chain mobility [150].

5.5. Mechanical properties

Incorporation of CNC in composites influenced their mechanical properties by improved filler-matrix compatibility and formation of filler network. The use of CNC as reinforcement phase in composites improved the stress-transfer efficiency of the composites and the overall mechanical properties. Tanpichai et al. developed a CNC reinforced poly (vinyl alcohol) (PVA) hydrogel using glutaraldehyde (GA) as a cross-linker. The maximum compressive strength of 53 kPa at 60% strain was obtained at 1 wt.% of CNC content. This compressive strength of composite hydrogels was 303% higher than the neat PVA hydrogel (17.5 kPa). Incorporation of CNC decreased the creep elasticity due to the restriction in the movement of molecular chains. The almost complete strain recovery (~97%) was observed for CNC incorporated hydrogels after fixed load removal for 15 min, compared to the 92% strain recovery of the cross-linked neat PVA hydrogels. Improved interaction between polymer matrix and CNCs contributed for efficient stress transfer from matrix to the reinforcements. At low CNC loading (below 1

wt%), the covalent bonds influenced the stress transfer of crosslinked hydrogels. However, at higher CNC loading, the free hydroxyl groups of polymer matrix and CNC formed hydrogen bonding among themselves. The combined effect of covalent and hydrogen bonding helped to improve the mechanical properties of the crosslinked hydrogels [124]. Dhar et al. produced a thermally recyclable poly (lactic acid) (PLA) grafted CNC (PLA-g-CNC) composite films. The grafted PLA chains provided a shielding effect to the sulfate and hydroxyl groups presented on the surface of CNCs. Due to this crosslinking, there was an improvement in stress transfer observed from CNC to PLA matrix. The tensile strength and Young's modulus were increased to ~40% and ~490%, respectively [127]. Yue et al. produced a biobased epoxy nanocomposite using amino silane functionalized CNC as reinforcing agent. The incorporation of these surface modified CNC in the epoxy nanocomposites improved their thermo-mechanical properties more than 7 times. The storage modulus at 160 °C was 151.5 MPa for the composite with 10 wt.% modified CNC, which was much higher compared to the 19.5 MPa for the neat resin [151]. The reaction between the amino functional groups on the surface of the modified CNC and the epoxy groups of the matrix facilitated the filler network formation and increased filler-matrix compatibility, which enhanced the thermomechanical properties [199]. Zhang et al. grafted poly (methyl methacrylate) (PMMA) and poly (butyl acrylate) (PBA) onto the surface of CNCs and used this modified CNC (MCNC) to reinforce the nanocomposites of PBA-co-PMMA. The nanocomposites treated with 7 wt.% MCNC showed 25 times increase in Young's modulus value and 3 times increase in tensile strength, compared to the neat PBA-co-PMMA. The good interfacial compatibility due to the incorporation of MCNC as reinforcement and improvement in chain entanglements between MCNCs and PBA-co-PMMA matrix contributed to improve the mechanical properties of the nanocomposites. The storage modulus value of neat PBA-co-PMMA at 42 °C was 4.82 MPa, which increased almost 4 times (22.60 MPa) with the incorporation of 7 wt.% MCNCs [117]. Pinheiro studied the effects of isocyanate modified CNC on the mechanical properties of poly (butylene adipate-co-terephthalate) (PBAT) nanocomposites. The amount of CNC was varied from 3, 5 to 7 wt.% in the composites. Addition of 5 and 7 wt% MCNC showed a significant increase in the Young's modulus of the composites, almost 12 and 42% higher compared to the neat PBAT. The tensile stress showed a declining trend with the increase in the filler amount, reaching to a 77% drop when the filler amount was 7 wt.%, compared to the neat PBAT results. There was a 30% increase in the elongation at break with 3 wt.% of MCNC incorporated composites compared to neat PBAT. The uniform dispersion of the nanoscale reinforcement in the matrix and subsequent CNC-polymer network formation aided in higher strain [152]. Butron et al. reinforced poly (ethylene brassylate) (PEB), a novel biodegradable polymer, with CNC to improve the mechanical properties of the composites. Addition of CNC up to 5 wt.% increased the ductility of the composites, though the trend reversed when the filler amount was increased. The composites loaded with CNC up to 20 wt.% retained the original ductile behavior of neat PEB, showing rupture elongations above 500%. However, the composites loaded with CNC over 30 wt.% exhibited a fragile behavior, breaking immediately after the yield point. An increasing stiffness was observed with the increase in CNC loading, indicated by the increase in the slope of the elastic region. For the 50 wt.% loading of CNCs, the Young's modulus showed a significant increase (150%) in its value, but the composites became very brittle [153].

There are several other examples [136,138,154–156] of the effect of CNC incorporation on the mechanical properties of the composites. The mechanical properties of different CNC based composites are listed below in Table 5. In almost all cases, a significant increase in Young's modulus and tensile strength were observed, with the increasing amount of CNC loading. However, after a certain point, the trend was reversed. This was due to the decrease in degree of dispersion and increased agglomeration of CNCs in the composites. The effective stress transfer was hindered due to increased agglomeration of reinforcing agents (CNCs). Following these examples, further research must be conducted to facilitate the dispersion of CNCs in polymer matrix and thereby increase in the mechanical properties of the resultant composites.

6. Cellulose nanocomposite applications

Cellulose nanocrystals are considered as sustainable alternative for inorganic and mineral nanofillers and have achieved approval for a wide range of applications which are summarized in this section. Due to the promising mechanical characteristics and facile modification of CNC, the most important application of CNC is the reinforcement of thermoplastic nanocomposites. In which, a broad range of polymers have been reported as the host matrix for different applications, including:

6.1. Packaging

Food packaging materials not only protect food from interfering or contamination from physical, chemical, and biological resources, but also extend the shelf life and nutrition capacity of food by hindering the migration of low-molecular weight compounds. Polymer materials, which are extensively employed in packaging materials do not exhibit absolute barriers against small molecules such as water vapor, gases and organic substances, and their barrier deficit may negatively impact their suitability for a specific application. Several approaches have been investigated to address such polymer matrices' drawbacks. One of the frequently used techniques to improve the barrier properties of polymer matrices is the use of CNC as reinforcing agents and permeability improvers. Over the past few decades, a large number of scientists incorporated CNC into a wide range of polymers to develop high performance nanocomposite films with application in food packaging sector, and some broad directions for the improvement of packaging materials containing CNC have been well reported in literature. In this regard, Yadav et al. showed that the addition of 1, 3, 5, and 7 wt.% CNC into f κ-carrageenan containing glycerol films reduced WVP by 52%, mainly due to the physical barrier by CNC to the passage of water through packaging film. However, higher concentration of CNC (9 wt.%) resulted in the formation of micro-scale aggregates and this in turn, resulted to a noticeable increase in permeability in nanocomposite films [157]. In a different study, incorporation of CNC into PHBV resulted in a strong interfacial interaction between polymer matrix and CNC, and restricted polymer chain mobility. Hence water vapor barrier properties improved to a noticeable degree [158]. Salmieri et al. developed an antimicrobial nanocomposite films containing oregano essential oil in PLA-CNC nanocomposite for storing mixed vegetables. The antimicrobial capacity of nanocomposite films against Listeria monocytogenes were evaluated and a quasi-total inhibition of bacteria was observed at day 14. The high antimicrobial properties of nanocomposite films against food borne pathogens were mainly attributed to the presence of volatile compounds found in well dispersed essential oil. While the addition of CNC resulted in an improvement in water adsorption from packed food, and this, in turn increased the tensile strength of nanocomposite films [159].

Cellulose nanostructures have been mainly applied as reinforcing agent, but they may also be used as moisture-absorber in packed food as excess moisture can result in microbial growth and food spoilage. In this regard, Oliverira et al. employed CNC from oat and eucalyptus to prepare aerogel as absorber in food packaging sector. They observed lower water absorption in eucalyptus-based CNC aerogel due to great pore size. However, the higher level of crystallinity in eucalyptus-based CNC aerogel induces the barrier effect of aerogel against diffusion of water and lower the water absorption. Therefore, the aerogels containing CNC with low level of crystallinity were introduced as moisture absorbers in food packaging mostly in meat packaging to decrease water condensation [160].

Table 6 represents the overview of the application of CNC in combination with different polymer matrices in food packaging industry.

Table 5
Summary of the mechanical properties of different CNC based composites.

Composition		Mechanical properties			Ref.
Host polymer	CNC content	Young's modulus (MPa)	Elongation at break (%)	Tensile strength (MPa)	
PBA-co-PMMA	0 wt% MCNC	2.25 ± 0.20	2099.19 ± 104.48	2.63 ± 0.63	[166]
	1 wt% MCNC	3.77 ± 0.56	1868.99 ± 182.89	3.34 ± 0.54	
	5 wt% MCNC	7.48 ± 0.55	1608.15 ± 65.20	6.27 ± 0.58	
	7 wt% MCNC	53.46 ± 2.14	980.14 ± 66.19	9.89 ± 1.01	
	10 wt% MCNC	65.88 ± 0.73	278.88 ± 52.5	6.79±0.50	
Neat PBAT	0	55.7 ± 2.0	544.5 ± 113.4	22.0 ± 3.7	[200]
	3 wt% MCNC	55.0 ± 1.7	710.6 ± 67.2	21.5 ± 2.1	
	5 wt% MCNC	62.3 ± 3.6	632.6 ± 58.6	13.5 ± 0.8	
	7 wt% MCNC	79.2 ± 2.0	567.4 ± 38.7	12.4 ± 0.7	
PEB	0	410 ± 19	613 ± 66	-	[201]
	2.5 wt%	469±12	751 ± 92	-	
	5.0 wt%	448 ± 11	759±50	-	
	10 wt%	501 ± 17	657 ± 64	-	
	20 wt%	599±59	521 ± 228	-	
	30 wt%	849 ± 55	178 ± 168	-	
	40 wt%	952 ± 65	63 ± 61	-	
	50 wt%	1040 ± 40	13 ± 6	-	
Gelatin nanofibers	0	161.8 ± 24.4	7.06 ± 2.12	4.21 ±0.54	[203]
	2.5 wt%	282.3 ± 36.2	6.42 ± 0.49	7.26± 0.49	
	5 wt%	545.3 ± 110.7	3.41 ± 0.90	11.20 ± 0.90	
	7.5 wt%	270.1 ± 68.4	3.59 ± 1.13	5.45 ± 1.35	
	10 wt%	249.4 ± 48.4	2.38 ± 0.28	4.54 ± 1.03	
	15 wt%	235.6 ± 36.8	1.74 ± 0.31	3.28 ± 0.43	

6.2. Biomedical

In recent years, there has been an increasing concern towards the application of natural polymers in biomedical fields. Among different natural polymers, biodegradable and biocompatible CNC with promising physical and chemical characteristics such as low toxicity, low density (1.6 g/cm3), high specific surface area, and high mechanical properties (elastic modulus of 110–220 GPa, ultimate tensile strength of 7.5 GPa) draws significant interest from many research communities. This section aims at summarizing the most recent advances in CNC and their composites with potential applications in biomedical engineering such as drug delivery, wound dressings, and tissue engineering. The major challenges and problems available in the application of CNC in biomedical field are discussed, while possible approaches to overcome issues are discussed.

6.2.1. Drug delivery

During the past decade, scholars continued to focus on several approaches such as compression, spray and dip coating, and encapsulation in the pharmaceutical sector to load polymeric structures with specific drug for targeted delivery and/or controlled release. It is highly recommended to encapsulate the drug with coating materials to achieve sustainable controlled release in a specific period [168]. In general, drug release depends upon the principle of diffusion phenomenon and comprises of three successive steps including absorbing liquid from gastrointestinal environment, swelling of the active elements in the drug, and drug collapsing [169].

The recent works disclose the potential of CNC as a suitable pharmaceutical excipient and carrier in drug delivery system, owing to their high specific surface area, colloidal stability, negative charge density, and promising mechanical properties. The unique characteristics of CNC allow loading charged and neutral drugs, controlled releasing of active compounds, and transporting drug to target cells [170,171]. In a work by Chen et al., electrospun composite membranes made of PHBV was reinforced by PDMAEMA grafted CNC for customized and long-term sustained release of a model drug in response to -g-PDMAEMA. The electrostatic interaction between composite membrane and negatively charged cancer cell accelerated *in vitro* uptake of drug for the tumor tissues, however, the aggregation of CNC at pH of 8 hindered the drug release [172] (Fig. 8).

Beside hydrophilic nature of CNC, chiral nematic structure of CNC which allows the formation of porous structure is another reason for using CNC as drug excipients [173], especially in the form of hydrogels. The employment of CNC in porous hydrogel can facilitate drug absorbing and dissolution process mainly due to their robust hydrophilic nature and swelling behavior in the presence of water. Due to high permeability, CNC hydrogels have extensity employed in different works to convert chemical, pH [174], thermal [175] and electrical signals into spontaneously conformational changes for triggering drug release in CNC hydrogels, while pH was the most predominant ones.

Ooi et al. successfully prepared stimuli-responsive semi-IPN gelatin-CNC hydrogels to respond to changes in pH. In this research, glutaraldehyde was employed as a cross-linker and different CNC concentrations was incorporated into gelatin-glutaraldehyde to control the hydrogel response against pH for theophylline loading and release. The incorporation of pristine CNC with high hydrophilicity character controlled the porous microstructure of the hydrogels, altering the swelling behavior and the drug- delivery kinetics at different pH values. The drug release profile of the CNC-gelatin hydrogels confirmed the capability of CNC-gelatin hydrogel to respond to different pH values and control drug release [176].

Nevertheless, the hydrophilic nature and highly negative surface restrict the application of virgin CNC for hydrophobic drugs (such as anticancer agents). Therefore, further surface modification treatments of CNC can manipulate their properties for binding the non-ionized or hydrophobic drugs which would not normally be bound to virgin CNC. In this regard, Castro et al. made an attempt to functionalize CNC with β-cyclodextrin (β -CD) to apply new active materials on the surface of CNC and allow the release of antibacterial molecules over a long period of time. In a different work, CNC surface was functionalized using propargyl groups for preparing nanomedicine of radionuclides for radio immune therapy (Fig. 9). In this work, oligoethylene glycol methacrylate and aminopropylmethacrylamide were incorporated to CNC to form a small number of primary amine pendant groups capable of carrying drugs. Nontoxic nature of functionalized CNC was demonstrated in a human ovarian cancer cell line and a human breast cancer cell line. The cellular uptake behavior of CNC conjugates as a critical factor in nanomedicines showed that CNC conjugates were uptake by ovarian cancer cell line. While, human breast cancer cell line showed lower intension in up taking CNC conjugates [177].

Table 6
Examples of CNC nanocomposite in food packaging sector.

CNC content	Polymer matrix	Thickness	RH(%)	Oxygen barrier property	Property	Ref.
30	Edible coating on alginate film	-	0 50 70	92 (ml.μm/m^{2}d^{-1}) 250 1427	Low oxidation of lipids of chicken during the first 3 days of storage	[161]
20	Gellan gum and glycerol coating	-	-		Constant color in coated mushroom for first 20 days Higher firmness in coated mushrooms Lower reduction in cap diameter	[162]
4	PET film	1 μm.	0 20 40 60 70 80	0.38 (ml.m^{-2}d^{-1}bar^{-1}) 1.03 2.05 23.07 56.41 83.97	Lower CO_2 barrier at high relative humidity	[163]
0.2	Hybrid PVA-cellulose bioactive aerogels	-	-	0.38 (ml.m^{-2}d^{-1}bar^{-1})	Controlled release of bioactive compounds improved water sorption; integrity of materials in water	[131]
1.2 2.4 3.6	Chitosan-nano clay film	40 μm	50	8.1 (ml.m^{-2}.d^{-1}.atm^{-1}) 5.4 7.2	Improved strength and tensile modulus Improved thermal stability Reduction in WV and OTR	[164]
1 3 5	Kappa-Carrageenan	-	-	18.5 (ml/mm^2/day) 11 15	Higher tensile and modulus strength Lower elongation at break Reduced oxygen transmission rate	[165]
5 7 11	Starch-glycerol-f montmorillonite film	-	-	35.26 (ml.m^{-1}.d^{-1}.Pa^{-1}) 37 38.5	Improvement in tensile strength and tensile modules Improvement in barrier properties Increment in disintegrability	[166]
1 5	PLA-Ag	200–220 μm	-	16.5 (ml.mm.m^{-2}day^{1}) 17.8	Increased the overall crystallinity Efficient barrier effect Reduction in water vapor permeability	[167]

6.2.2. Wound dressing

Wound dressing materials are designed to support the wound via providing a barrier against bacterial penetration, endorse gaseous diffusion, treating wound infections, and promoting wound healing. Appropriate wound dressing with adequate moisture retention properties also provide a proper media hindering the moisture loss from wound thus facilitating and accelerating the healing process. The last decades have witnessed rising interest in using naturally occurring polymers and their corresponding hybrids in the field of wound dressing materials due to their biocompatibility, biodegradability, and relatively low cytotoxicity. Among different natural polymers, CNC found their application in wound dressing materials as either reinforcing agent [178] or main building block due to their wide availability and outstanding mechanical properties [179]. Wound dressing materials derived directly from CNC can be constructed in form of film, hydrogel pads, or injectable hydrogels. The CNC-based wound dressing materials can be modified via incorporating active molecules such as antimicrobial drugs, antioxidants, hormones, enzymes, and vitamins to induct self-healing behavior into CNC-based wound dressing system.

In one effort, Zhang et al. developed an injectable self-healing nanocomposite hydrogel made of modified CNC and carboxymethyl chitosan (CMC) to absorb and retain the wound exudate and sustain an ideal moist environment for deep burn wound beds. They employed periodate oxidation to obtain dialdehyde CNC (DACNC) and the hydrogels were cross-linked by dynamic Schiff-base linkages between amines from carboxymethyl chitosan and DACNC. The result of healing process showed that CMC-DACNC hydrogels showed higher self-healing behavior than chitosan-based ones owing to the reinforcing effect of DACAC as well as their role as a chemical cross-linker (Fig. 10) [180].

In a different study, Tong et al. proposed a facile method synthesizing CNC films serving as antimicrobial drug delivery system in a diabetic wound dressing. PVA-CNC films were loaded with curcumin via solvent

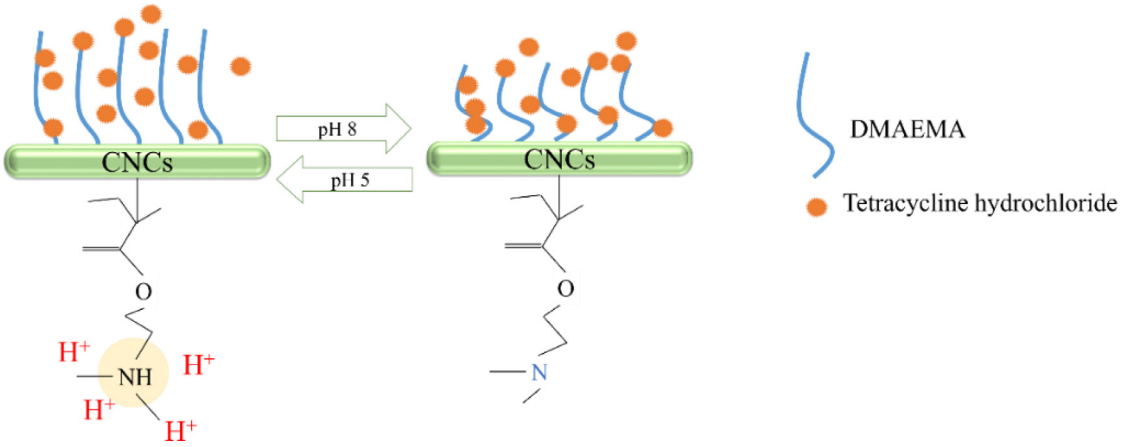

Fig. 8. *In vitro* drug release profiles of PHBV/CNC-g-PDMAEMA at different pH. PDMAEMA grafted CNC reinforced composite membranes for customized and long-term sustained release of a model drug. (Reproduced with permission from [172]).

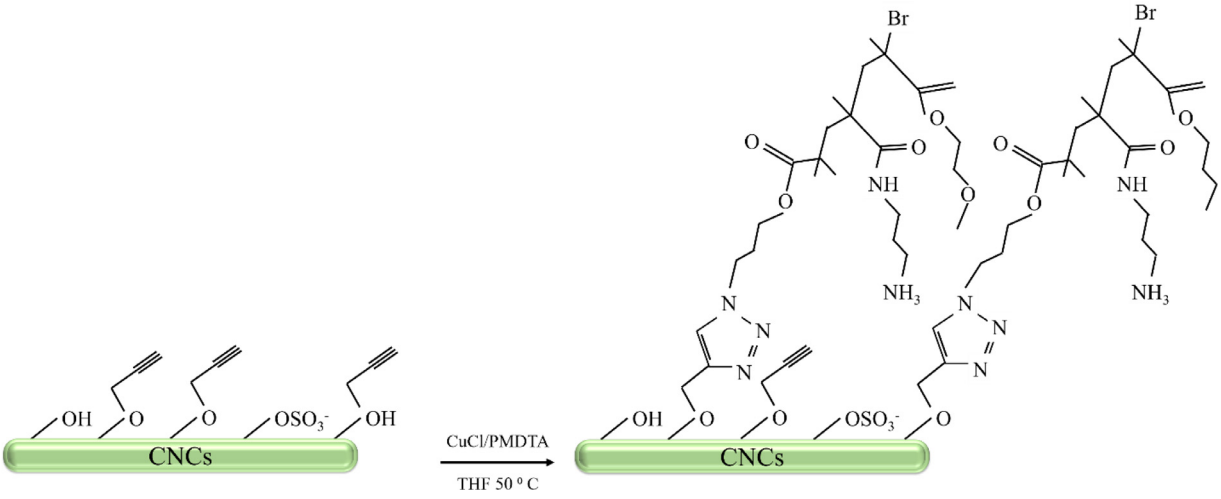

Fig. 9. schematic diagram of CNC functionalization using propargyl groups to be used as nanomedicine (Reproduced with permission from [177]).

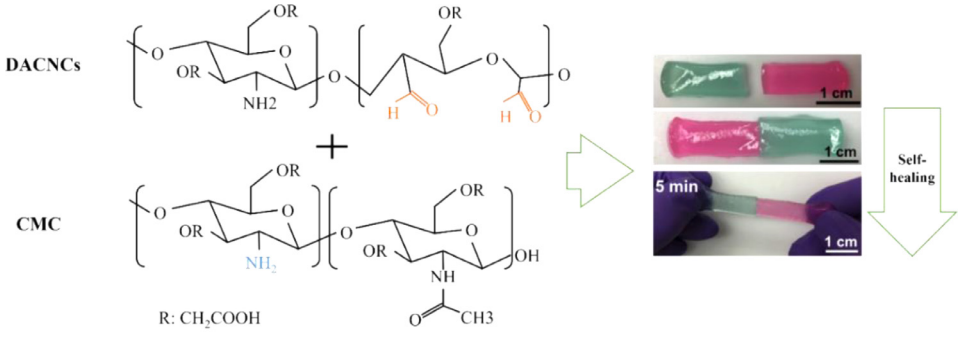

Fig. 10. Gel formation and self-healing process of CMC-DACNC. (Reproduced with permission from [180]).

casting method. The presence of CNC resulted in a robust binding of curcumin to PVA-CNC film, which hinder losing curcumin through washing. Curcumin loaded CNC film meaningfully enhanced wound healing process of diabetic rat models, with full thickness skin wound [181].

Hemocompatibility and hemolysis testing are considered as important testing assays for proper wound dressing materials. The former one explains the interactions of wound dressing material with blood for adverse effects arising from the exposure of the foreign material to toward red blood cells and proteins in an open wound, and later one is the breakdown of red blood cells exposed to foreign materials [182].

In a comprehensive research conducted by Cheng et al. carboxyl groups were added to the surface of CNC via TEMPO treatment and TEMPO-mediated oxidized CNC and alginate formed composite films and sponges for absorbing wound exudate while Ca^{2+} was used as cross-linking agent. The composite films and sponges were employed to cover rabbit ear injury and blood loss of sponges was lower than that of films (Fig. 11). Their results showed that the composite components had no influence on physiological action of the blood cells while incubating composite materials with platelet rich plasma resulted in the platelets bond on composites surface, mainly due to the presence of carboxyl groups on modified CNC, hence attracted and activated the platelets

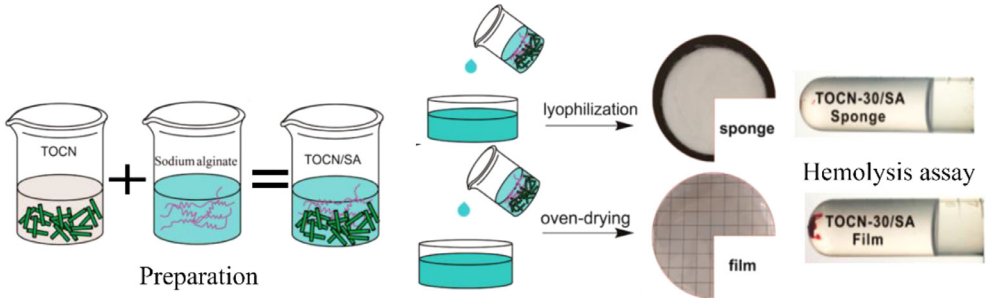

Fig. 11. Preparation and hemolysis analysis for film and sponge CNC- alginate composite. (Reproduced with permission from [183]).

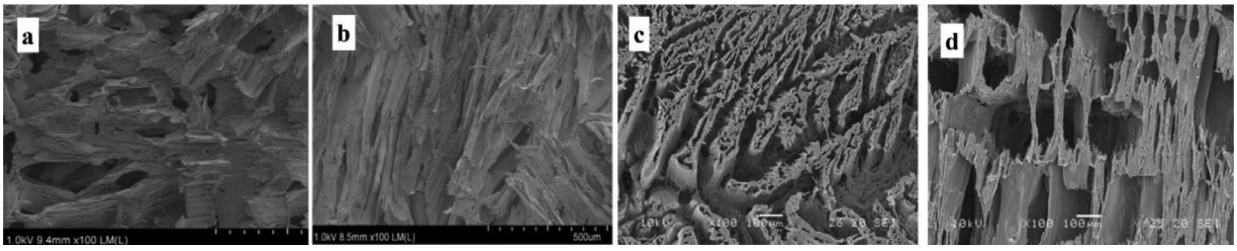

Fig. 12. SEM micrograph of hydrogel cross-sections; a) pure PVA, b) PVA-2 wt.% CNC, c) PVA-6 wt.% CNC (d), PVA-8 wt.% CNC (Reproduced with permission from [186]).

and led to a rapid hemostatic effect. They claimed that their composites especially sponges exhibited an outstanding hemocompatibility and could be considered as an appropriate wound dressing system [183].

6.2.3. Tissue engineering

The application of naturally occurred polymers in tissue engineering is an important emerging topic in biomedical engineering that developed mostly in the last decade. Low toxicity, low density, high aspect ratio, and most importantly promising mechanical characteristics make CNC an ideal candidate for composing functional tissue substitutes that can be used for reconstructing damaged tissues or organs [184].

In the field of tissue engineering, the design of a porous membrane with well-defined geometry and inter-connected pore structure capable of retaining bioactive peptides that enhance cell adhesion and neurite outgrowth is an important parameter in selecting proper artificial tissues of human or animal organ. According to several attempts in literatures, the hydrophilic hydroxyl moieties of CNC and their ability in forming a porous and soft membrane with multi and nanoscale open-pore architecture facilitate cell attachment and cell viability for recovering injured tissues or organs [185]. Lam et al. employed CNC obtained from sugarcane bagasse for synthesizing PVA/CNC porous nanocomposite scaffolds for cultivating human skin cells. They reported non-cytotoxic porous scaffolds with cell viability of 82% with pore size which was strongly controlled by CNC contents. The higher CNC contents resulted in an increase in pore size due to a reduction in the free PVA volume fraction (Fig. 12). The higher CNC content also resulted to an increase in swelling degree as CNC limited the polymer chain movement [186].

In a different approach, CNC were combined with collagen films to obtain corneal tissue scaffolds. The optical transparency of CNC-collagen films fulfilled the corneal tissue needs. Furthermore, corneal epithelial cells cultured on the CNC-collagen films exhibited a slightly faster proliferation rate than cells on collagen films and the addition of 5 and 7 wt.% CNC into collagen films promoted the epithelialization healing process (Fig. 13). The tensile strength and elastic modulus of CNC-collagen films were notably higher than those collagen films, mainly due to crosslinking role of CNC which increased the bridges, connected points, and strength of nanocomposite films [187].

Gao et al studied the effects combination of *in-situ* composite method and freeze-drying technique in fabricating synthetic bone tissue scaffolds with high compressive strength and wettability from gelatin-bioactive glass (BG-Gel) system. They reported that the 3D porous network with interconnecting pores improved surface hydrophilicity of nanocomposite scaffolds as CNC incorporation provided a suitable environment for cell-scaffold interaction, cell growth and proliferation in bone regeneration [188].

6.3. Energy

Energy supply, in all its forms, is considered as a leading prospect for a sustainable economic, cultural, and social development. Powering the future, the application of polymeric materials in the field of energy devices has been shifted to biopolymers such as CNC. The employment of CNC in different energy fields has attracted extensive attention in both industry and academia. Over the last few years, researchers have focused on the application of CNC-based nanocomposites in energy devices largely due to high cell capacitance, effective charge-discharge rate, stable cyclic performance, and piezoelectric properties. The main application of CNC-based nanocomposites in energy devices can be classified into organic photovoltaic (OPV) cells and super capacitors categories.

6.3.1. Organic photovoltaic (OPV) cells

OPV cells are solar cells with organic absorbing layers from either polymers or small molecules which can absorb the fluorescence and convert it to electricity. A number of efforts have been made to prepare homogenous CNC films with smooth surface as a substrate in OPV devices. Furthermore, transparency and light scattering are natural properties in CNC nanopapers which make CNC films desirable substrate for efficient OPV cells with light management. On the other hand, as strong hydrophobicity, and high mechanical characteristics are required for OPV cells, surface modification is an essential step in preparing CNC-based nanocomposites for OPV cells as evidenced by multiple reports [164,189]. Furthermore, CNC are electrical insulators and the employment of conductive materials while protecting the optical transparency of CNC nanopapers has been revealed to be practical and generated new materials with promising characteristics for photovoltaic applications [190]. In this regard, in a research by Hu et al., a conductive CNC layer was successfully prepared by depositing conductive materials including tin-doped indium oxide, carbon nanotubes and silver nanowire. The CNC nanopapers were spin-coated, and heat treated, and metal electrodes were thermally evaporated onto the film. The CNC nanopapers

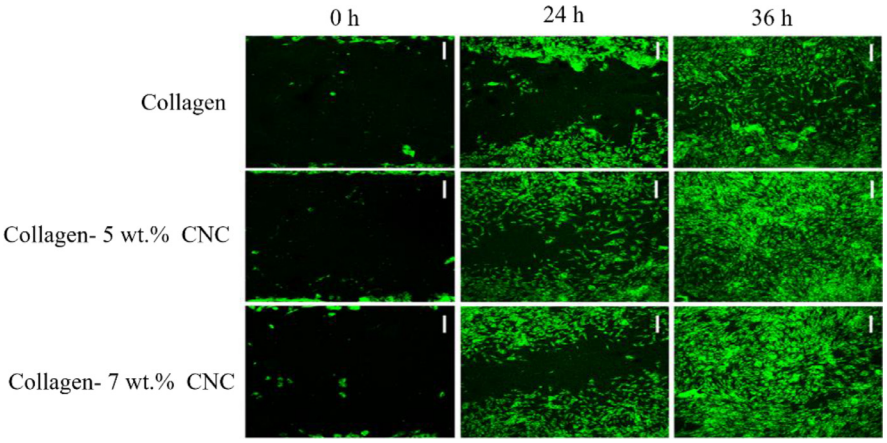

Fig. 13. Confocal laser scanning microscopy image of wound healing assays using corneal epithelial cells cultured on the collagen film and collagen - CNC films containing (Reproduced with permission from [187]).

were highly transparent and majority of the transmitted light scattered off in a normal direction since the size of the CNC was lower than wavelength of visible light. They also observed low angle dependency at a wide range of wavelengths, which can improve the cell's power conversion efficiency [191]. In a different study by Cheng et al., tough nanocomposite papers were prepared using tunicate CNC, and O-(2,3-Dihydroxypropyl) cellulose (DHPC). Tin-doped indium oxide was coated on CNC nanopaper using magnetron sputtering and the average roughness was as low as 4.4 nm. The transparent tunicate CNC nanopapers possessed power conversion efficiency of 4.98%, proving their function in optoelectronic devices [192].

6.3.2. CNC-based nanocomposites for super capacitors

Super capacitors, also known as electrochemical double-layer capacitors include materials with high capacity, and short charging cycle which can fill the gap between batteries and conventional capacitors. CNC itself are not electrical conductor, however they can be employed as an inherently recyclable and eco-friendly substances for composite super capacitors. In a study by Chen et al. metal nanoparticles (MNPs) were uniformly distributed on CNC to prepare core-shell structured melamine-formaldehyde (MF) coated CNC. Platinum and platinum between 1 and 2 nm in size were selected for the deposition on porous MFCNC. The addition of MF resin on CNC not only preserves CNC from oxidation, but also resulted in the formation of a high porosity and nitrogen functionalities that are favorable for additional metal deposition. The synthesized Pd/MFCNC exhibited excellent catalytic performance with a turnover frequency of 3168 h^{-1} mainly due to the small particle size and uniform MNP deposition attained from porous MFCNC [193]. In a different work, core-shell PPy/PVP/CNC nanorod were prepared via physical adsorption of PVP onto CNC surface to alter the hydrophilicity characteristics of CNC and favor the growth of pyrrole. They reported the conductivity of 36.9 S/cm for the composite material with 10% PVP to CNC mass ratio. Furthermore, an improvement of 35% in the specific capacitance was reported for core-shell system with high cycling stability at 0.1 V/s mainly due to uniform PPy deposition that accelerates the charge transfer and diffusion [194].

6.4. Smart materials

Recently, extensive study has been allotted to the development of renewable smart materials made with biobased materials such CNC [195]. The efficiency of CNC as functional resources for smart materials depends not only upon their capability to act as a stabilizing building block for bio-sensing elements, but also upon its large surface area, controlled morphology, and structure. Due to unique characteristics, CNC are suitable platform for immobilization of bioactive molecules. In which, the enzymes can be linked to CNC via covalent bonds, salt bridges or physical inclusion complexes [196,197]. In addition, diverse noncovalent surface modification treatments such as surfactants adsorption, sulfonation, silylation, amidation, TEMPO-mediated oxidation, esterification, etherification, urethanization, and polymer graphting can preferably alter the structure of CNC to specific functional groups. In general, CNC nanocomposite materials have been tested to respond to different external stimuli such as heat, pH, moisture, magnetic field and combination of stimuli like heat and pH at the same time.

Thermo-sensitive CNC nanocomposites are the most common smart nanocomposite in the literature. In which, lower critical solution temperature (LCST) or upper critical solution temperature (UCST) play the main role in adjusting nanocomposite response against temperature change via phase transition. LCST and UCST are critical temperatures which polymer solutions have different phase behavior and show different miscibility above or below these points. In this regards, an innovative and efficient approach were proposed by Kato et al. [198]. They prepared a mechanically robust, thermoresponsive, ion-conducting nanocomposite films from poly(2-phenylethylmethacrylate)-grafted CNC by solvent casting. Thermally induced conductivity response of nanocomposite films exhibited collapse of grafted PPMA chains and phase separation at temperatures above LCST. They claimed the potential application of the nanocomposite films in thermal cutoff safety devices such as thermal fuse where a reduction in conductivity at temperatures above LCST is needed.

Sun et al. reported temperature-sensitivity and optical tunability of CNC- PNIPAm hydrogels. They observed a notable change in micro/nano structures of hydrogel films when dried below and above the LCST. In particular, transparency or semi-transparency was observed below LCST while light scattering and hence opacity was observed above LCST. These observations were mainly due to solubility and hydrogen bonding of hydrophilic PNIPAm and CNC below and above LCST. The thermal responsivity studied via contact angle measurement also shown higher hydrophobic nature above LCST as polymer chains swell at temperatures below the LCST, while at higher temperatures, they collapse to expose hydrophobic regions [199].

The pH sensitivity of polymer solution is another mechanism studied for the development of smart materials in different fields. Generally, when variation of surface charge of materials corresponding to the changing of pH lead to different properties, those materials can be considered as pH sensitive materials. In the literature it was reported that in order to use CNC as a pH sensitive system some preliminary steps are required to introduce pH sensitive linkages to the surface of CNC. Surface functionalization and introducing carboxylate groups and amine groups [200,201] to the surface of CNC is one of the most common techniques introducing the pH sensitivity to CNC nanocomposite systems. Incorporation of CNC into inherently pH sensitive polymers is another technique employed for synthesizing pH sensitive CNC nanocomposites [41]. In general, various swelling and deswelling profile in hydrogels due to the formation of hydrogen bonds between water molecules and

hydrophilic components of hydrogel is the main response against different external stimuli. Incorporation of different functional groups such as amine groups on to the surface of CNC can result in different gelation behavior according to the pH gradient in the living body for target drug release [202] In particular, in pH sensitive CNC Hydrogels, the pores get smaller in acidic media, while, they grow at alkaline pH [203].

Even though a lot of progress has been made in the application of CNC in composites, many challenges still exist in the processing of CNC based polymer composites. Current research is focused on addressing agglomeration of CNCs during drying, interfacial compatibility, non-uniform dispersion and degradation during production of composites. Chemical surface modification treatments and physical dispersion strategies are showing promising results.

Declaration of Competing Interest

None

References

[1] T.C. Mokhena, M.J. John, Cellulose nanomaterials: new generation materials for solving global issues, Cellulose 27 (3) (2020) 1149–1194.
[2] A. Dufresne, Nanocellulose processing properties and potential applications, Current Forestry Reports 5 (2) (2019) 76–89.
[3] J. Shojaeiarani, D. Bajwa, A. Shirzadifar, A review on cellulose nanocrystals as promising biocompounds for the synthesis of nanocomposite hydrogels, Carbohydr. Polym. 216 (2019) 247–259.
[4] R. Dhumpa, J. Foster, High-Performance Nanocellulose Composite for Aviation and Aerospace, Innovatech Engineering LLC, Tallahassee, FLUnited States, 2018.
[5] K. Degirmenci, J.P. Shim, M.H. Breitner, F. Nolte, and J. Passlick, "Future of flexible work in the digital age: bring your own device challenges of privacy protection," 2019.
[6] H. Charreau, E. Cavallo, M.L. Foresti, Patents involving nanocellulose: analysis of their evolution since 2010„ Carbohydr. Polym. 237 (2020) 116039.
[7] S. Sinquefield, P.N. Ciesielski, K. Li, D.J. Gardner, S. Ozcan, Nanocellulose dewatering and drying: current state and future perspectives, ACS Sustain. Chem. Eng. (2020).
[8] "TAPPI Nano 2019: Focus on new markets – paper 360." https://paper360.tappi.org/2019/10/03/2346/ (accessed Nov. 28, 2020).
[9] K.J. De France, T. Hoare, E.D. Cranston, Review of hydrogels and aerogels containing nanocellulose, Chem. Mater. 29 (11) (2017) 4609–4631.
[10] B. Lyne, Market prospects for nanocellulose, The Royal Institute of Technology (2013).
[11] A. Dufresne, Cellulose nanomaterials as green nanoreinforcements for polymer nanocomposites, Philos. Trans. R. Soc. A 376 (2112) (2018) 20170040.
[12] F. Luzi, et al., Valorization and extraction of cellulose nanocrystals from North African grass: ampelodesmos mauritanicus (Diss), Carbohydrate Polym. 209 (2019) 328–337.
[13] X. Yang, H. Liu, F. Han, S. Jiang, L. Liu, Z. Xia, Fabrication of cellulose nanocrystal from Carex meyeriana Kunth and its application in the adsorption of methylene blue, Carbohydr. Polym. 175 (2017) 464–472.
[14] F.V. Ferreira, M. Mariano, S.C. Rabelo, R.F. Gouveia, L.M.F. Lona, Isolation and surface modification of cellulose nanocrystals from sugarcane bagasse waste: from a micro-to a nano-scale view, Appl. Surf. Sci. 436 (2018) 1113–1122.
[15] E. Abu-Danso, V. Srivastava, M. Sillanpää, A. Bhatnagar, Pretreatment assisted synthesis and characterization of cellulose nanocrystals and cellulose nanofibers from absorbent cotton, Int. J. Biol. Macromol. 102 (2017) 248–257.
[16] L.K. Kian, M. Jawaid, H. Ariffin, Z. Karim, Isolation and characterization of nanocrystalline cellulose from Roselle-derived microcrystalline cellulose, Int. J. Biol. Macromol. 114 (2018) 54–63.
[17] B. Li, et al., Cellulose nanocrystals prepared via formic acid hydrolysis followed by TEMPO-mediated oxidation, Carbohydr. Polym. 133 (2015) 605–612.
[18] M. Kunaver, A. Anžlovar, E. Žagar, The fast and effective isolation of nanocellulose from selected cellulosic feedstocks, Carbohydr. Polym. 148 (2016) 251–258.
[19] A.A. Oun, J.-W. Rhim, Isolation of cellulose nanocrystals from grain straws and their use for the preparation of carboxymethyl cellulose-based nanocomposite films, Carbohydr. Polym. 150 (2016) 187–200.
[20] Y.K. Dasan, A.H. Bhat, F. Ahmad, Polymer blend of PLA/PHBV based bionanocomposites reinforced with nanocrystalline cellulose for potential application as packaging material, Carbohydr. Polym. 157 (2017) 1323–1332.
[21] Y. Jiang, et al., Preparation of cellulose nanocrystals from Humulus japonicus stem and the influence of high temperature pretreatment, Carbohydr. Polym. 164 (2017) 284–293.
[22] R.M. Leão, P.C. Miléo, J.M. Maia, S.M. Luz, Environmental and technical feasibility of cellulose nanocrystal manufacturing from sugarcane bagasse, Carbohydr. Polym. 175 (2017) 518–529.
[23] S. Thambiraj, D.R. Shankaran, Preparation and physicochemical characterization of cellulose nanocrystals from industrial waste cotton, Appl. Surf. Sci. 412 (2017) 405–416.
[24] F. Kallel, F. Bettaieb, R. Khiari, A. García, J. Bras, S.E. Chaabouni, Isolation and structural characterization of cellulose nanocrystals extracted from garlic straw residues, Ind. Crops Prod. 87 (2016) 287–296.
[25] E. Fortunati, et al., Revalorization of barley straw and husk as precursors for cellulose nanocrystals extraction and their effect on PVA_CH nanocomposites, Ind. Crops Prod. 92 (2016) 201–217.
[26] Y. Wang, et al., Homogeneous isolation of nanocellulose from eucalyptus pulp by high pressure homogenization, Ind. Crops Prod. 104 (2017) 237–241.
[27] R. Dungani, et al., Preparation and fundamental characterization of cellulose nanocrystal from oil palm fronds biomass, J. Polym. Environ. 25 (3) (2017) 692–700.
[28] J.W. Rhim, J.P. Reddy, X. Luo, Isolation of cellulose nanocrystals from onion skin and their utilization for the preparation of agar-based bio-nanocomposites films, Cellulose 22 (1) (2015) 407–420.
[29] K. Song, X. Zhu, W. Zhu, X. Li, Preparation and characterization of cellulose nanocrystal extracted from Calotropis procera biomass, Bioresour. Bioprocess. 6 (1) (2019) 1–8.
[30] A. Nkalane, O.A. Oyewo, T. Leswifi, M.S. Onyango, Application of coagulant obtained through charge reversal of sawdust-derived cellulose nanocrystals in the enhancement of water turbidity removal, Mater. Res. Express 6 (10) (2019) 105060.
[31] T.P. Lambrou, C.C. Anastasiou, C.G. Panayiotou, A nephelometric turbidity system for monitoring residential drinking water quality, in: Proceedings of the International Conference on Sensor Applications, Experimentation and Logistics, 2009, pp. 43–55.
[32] M. Shimizu, et al., Fast and robust nanocellulose width estimation using turbidimetry, Macromol. Rapid Commun. 37 (19) (2016) 1581–1586.
[33] T. Phan-Xuan, A. Thuresson, M. Skepö, A. Labrador, R. Bordes, A. Matic, Aggregation behavior of aqueous cellulose nanocrystals: the effect of inorganic salts, Cellulose 23 (6) (2016) 3653–3663.
[34] Y. Xu, "Rheology and structure of aqueous nanocrystalline cellulose suspensions," 2019.
[35] S.S. Singh, D.R. Salem, R.K. Sani, Spectroscopy, microscopy, and other techniques for characterization of bacterial nanocellulose and comparison with plant-derived nanocellulose, in: Microbial and Natural Macromolecules, Elsevier, 2021, pp. 419–454.
[36] S. Ozkar, et al., Sustainable Preparation of Metal Nanoparticles: Methods and Applications, Royal Society of Chemistry, 2012.
[37] M.C. Li, C. Mei, X. Xu, S. Lee, Q. Wu, Cationic surface modification of cellulose nanocrystals: toward tailoring dispersion and interface in carboxymethyl cellulose films, Polymer 107 (2016) 200–210.
[38] M.S. Reid, T.C. Stimpson, E. Niinivaara, M. Villalobos, E.D. Cranston, Comparing soft semicrystalline polymer nanocomposites reinforced with cellulose nanocrystals and fumed silica, Ind. Eng. Chem. Res. 57 (1) (2018) 220–230.
[39] J.D. Clogston, A.K. Patri, Zeta potential measurement,", in: Characterization of Nanoparticles Intended for Drug Delivery, Springer, 2011, pp. 63–70.
[40] S.P. Akhlaghi, et al., Synthesis of amine functionalized cellulose nanocrystals: optimization and characterization, Carbohydr. Res. 409 (2015) 48–55.
[41] W. Li, B. Ju, S. Zhang, Novel amphiphilic cellulose nanocrystals for pH-responsive Pickering emulsions, Carbohydr. Polym. 229 (2020) 115401.
[42] R. Prathapan, R. Thapa, G. Garnier, R.F. Tabor, Modulating the zeta potential of cellulose nanocrystals using salts and surfactants, Colloids Surf. A 509 (2016) 11–18.
[43] J. Lv, G. Zhang, H. Zhang, F. Yang, Graphene oxide-cellulose nanocrystal (GO-CNC) composite functionalized PVDF membrane with improved antifouling performance in MBR: behavior and mechanism, Chem. Eng. J. 352 (2018) 765–773.
[44] M. Kaushik, C. Fraschini, G. Chauve, J.L. Putaux, A. Moores, Transmission electron microscopy for the characterization of cellulose nanocrystals, Transm. Electron Microsc. Theory Appl. (2015).
[45] L.C. da Silva, A. Cassago, L.C. Battirola, M. do Carmo Gonçalves, R.V. Portugal, Specimen preparation optimization for size and morphology characterization of nanocellulose by TEM, Cellulose 27 (9) (2020) 5435–5444.
[46] C. Campano, A. Balea, Á. Blanco, C. Negro, A reproducible method to characterize the bulk morphology of cellulose nanocrystals and nanofibers by transmission electron microscopy, Cellulose 27 (9) (2020) 4871–4887.
[47] Y. Ogawa, J.L. Putaux, Transmission electron microscopy of cellulose. Part 2: technical and practical aspects, Cellulose 26 (1) (2019) 17–34.
[48] Y. He, Y. Boluk, J. Pan, A. Ahniyaz, T. Deltin, P.M. Claesson, Corrosion protective properties of cellulose nanocrystals reinforced waterborne acrylate-based composite coating, Corros. Sci. 155 (2019) 186–194.
[49] H. Lu, Y. Gui, L. Zheng, X. Liu, Morphological, crystalline, thermal and physicochemical properties of cellulose nanocrystals obtained from sweet potato residue, Food Res. Int. 50 (1) (2013) 121–128.
[50] M. Kaushik, C. Fraschini, G. Chauve, J.L. Putaux, A. Moores, Transmission electron microscopy for the characterization of cellulose nanocrystals, Transm. Electron. Microsc. Theory Appl. (2015).
[51] Y.M. Kim, et al., Cationic cellulose nanocrystals complexed with polymeric siRNA for efficient anticancer Drug delivery, Carbohydr. Polym. 247 (2020) 116684.
[52] M. Shariatzadeh, D. Grecov, Aqueous suspensions of cellulose nanocrystals as water-based lubricants, Cellulose 26 (7) (2019) 4665–4677.
[53] W.P.F. Neto, Morphological investigation of cellulose nanocrystals and nanocomposite applications (Doctoral dissertation, Universidade Federal de Uberlândia) (2017).
[54] S. Imlimthan, et al., Systematic *in vitro* biocompatibility studies of multimodal cellulose nanocrystal and lignin nanoparticles, J. Biomed. Mater. Res. Part A 108 (3) (2020) 770–783.

[55] J. Leboucher, et al., High-yield cellulose hydrolysis by HCl vapor: Co-crystallization, deuterium accessibility and high-temperature thermal stability, Cellulose (2020) 1–21.
[56] C.J. Saelices, M. Save, I. Capron, Synthesis of latex stabilized by unmodified cellulose nanocrystals: the effect of monomers on particle size, Polym. Chem. 10 (6) (2019) 727–737.
[57] M. Li, et al., Thermo-thickening drilling fluids containing bentonite and dual-functionalized cellulose nanocrystals, Energy Fuels 34 (7) (2020) 8206–8215.
[58] L. Di Giorgio, L. Martín, P.R. Salgado, A.N. Mauri, Synthesis and conservation of cellulose nanocrystals, Carbohydr. Polym. 238 (2020) 116187.
[59] B. Huang, H. He, H. Liu, Y. Zhang, X. Peng, B. Wang, Multi-type cellulose nanocrystals from sugarcane bagasse and their nanohybrids constructed with polyhedral oligomeric silsesquioxane, Carbohydr. Polym. 227 (2020) 115368.
[60] H. Doh, M.H. Lee, W.S. Whiteside, Physicochemical characteristics of cellulose nanocrystals isolated from seaweed biomass, Food Hydrocolloids 102 (2020) 105542.
[61] Z. Wang, et al., Isolation and characterization of cellulose nanocrystals from pueraria root residue, Int. J. Biol. Macromol. 129 (2019) 1081–1089.
[62] M. Chemin, C. Moreau, B. Cathala, A. Villares, Asymmetric modification of cellulose nanocrystals with PAMAM dendrimers for the preparation of pH-responsive hairy surfaces„ Carbohydr. Polym. 249 (2020) 116779.
[63] P. Bagde, N. Vigneshwaran, Improving the stability of bacteriocin extracted from enterococcus faecium by immobilization onto cellulose nanocrystals, Carbohydr. Polym. 209 (2019) 172–180.
[64] E.J. Foster, et al., Current characterization methods for cellulose nanomaterials, Chem. Soc. Rev. 47 (8) (2018) 2609–2679.
[65] E. Espino, M. Cakir, S. Domenek, A.D. Román-Gutiérrez, N. Belgacem, J. Bras, Isolation and characterization of cellulose nanocrystals from industrial by-products of Agave tequilana and barley, Ind. Crops Prod. 62 (2014) 552–559.
[66] F. Hemmati, S.M. Jafari, R.A. Taheri, Optimization of homogenization-sonication technique for the production of cellulose nanocrystals from cotton linter, Int. J. Biol. Macromol. 137 (2019) 374–381.
[67] L. Pinďáková, V. Kašpárková, R. Bordes, Role of protein-cellulose nanocrystal interactions in the stabilization of emulsion, J. Colloid Interface Sci. 557 (2019) 196–206.
[68] M. Uhlig, et al., Two-dimensional aggregation and semidilute ordering in cellulose nanocrystals, Langmuir 32 (2) (2016) 442–450.
[69] A. Mtibe, T.C. Mokhena, S. Muniyasamy, O. Ofosu, M.J. Mochane, 15 recent developments in textile-reinforced composites and biocomposites, Fibres Smart Text. Adv. Manuf. Technol. Appl. (2019) 291.
[70] V. Favier, G.R. Canova, J.Y. Cavaillé, H. Chanzy, A. Dufresne, C. Gauthier, Nanocomposite materials from latex and cellulose whiskers, Polym. Adv. Technol. 6 (5) (1995) 351–355.
[71] J. Shojaeiarani, D. Bajwa, G. Holt, Sonication amplitude and processing time influence the cellulose nanocrystals morphology and dispersion, Nanocomposites 6 (1) (2020) 41–46.
[72] V. Heshmati, M.R. Kamal, B.D. Favis, Tuning the localization of finely dispersed cellulose nanocrystal in poly (lactic acid)/bio-polyamide11 blends, J. Polym. Sci. Part B Polym. Phys. 56 (7) (2018) 576–587.
[73] N.H. Inai, A.E. Lewandowska, O.R. Ghita, S.J. Eichhorn, Interfaces in polyethylene oxide modified cellulose nanocrystal-polyethylene matrix composites, Compos. Sci. Technol. 154 (2018) 128–135.
[74] S. Eyley, W. Thielemans, Surface modification of cellulose nanocrystals, Nanoscale 6 (14) (2014) 7764–7779.
[75] M. Mariano, N. El Kissi, A. Dufresne, Cellulose nanocrystals and related nanocomposites: review of some properties and challenges, J. Polym. Sci. Part B Polym. Phys. 52 (12) (2014) 791–806.
[76] K. Sahlin, L. Forsgren, T. Moberg, D. Bernin, M. Rigdahl, G. Westman, Surface treatment of cellulose nanocrystals (CNC): effects on dispersion rheology, Cellulose 25 (1) (2018) 331–345.
[77] L. Timhadjelt, A. Serier, M.N. Belgacem, J. Bras, Elaboration of cellulose based nanobiocomposite: effect of cellulose nanocrystals surface treatment and interface 'melting, Ind. Crops Prod. 72 (2015) 7–15.
[78] M.S. Islam, L. Chen, J. Sisler, K.C. Tam, Cellulose nanocrystal (CNC)–inorganic hybrid systems: synthesis, properties and applications, J. Mater. Chem. B 6 (6) (2018) 864–883.
[79] J. Sitompul, D. Setyawan, D.Y.J. Kim, H.W. Lee, Synthesis of PDLLA/PLLA-bentonite nanocomposite through sonication, AIP Conf. Proc. 1725 (1) (2016) 020080.
[80] S. Pradhan, J. Hedberg, E. Blomberg, S. Wold, I.O. Wallinder, Effect of sonication on particle dispersion, administered dose and metal release of non-functionalized, non-inert metal nanoparticles, J. Nanopart. Res. 18 (9) (2016) 285.
[81] J. Shojaeiarani, D.S. Bajwa, K. Hartman, Mechanical Techniques for enhanced dispersion of cellulose nanocrystals in polymer matrices, in: Sustainable Polymer Composites and Nanocomposites, Springer, 2019, pp. 437–449.
[82] F. Yetiş, X. Liu, W.W. Sampson, R.H. Gong, Acetylation of lignin containing microfibrillated cellulose and its reinforcing effect for polylactic acid, Eur. Polym. J. 134 (2020) 109803.
[83] J.C. Natterodt, A. Shirole, J. Sapkota, J.O. Zoppe, C. Weder, Polymer nanocomposites with cellulose nanocrystals made by co-precipitation, J. Appl. Polym. Sci. 135 (24) (2018) 45648.
[84] Y. Mao, et al., Phase separation and stack alignment in aqueous cellulose nanocrystal suspension under weak magnetic field, Langmuir 34 (27) (2018) 8042–8051.
[85] B. Frka-Petesic, H. Radavidson, B. Jean, L. Heux, Dynamically controlled iridescence of cholesteric cellulose nanocrystal suspensions using electric fields, Adv. Mater. 29 (11) (2017) 1606208.
[86] A. Kaboorani, B. Riedl, Surface modification of cellulose nanocrystals (CNC) by a cationic surfactant, Ind. Crops Prod. 65 (2015) 45–55.
[87] H. Patil, R.V. Tiwari, M.A. Repka, Hot-melt extrusion: from theory to application in pharmaceutical formulation, Aaps Pharmscitech 17 (1) (2016) 20–42.
[88] S. Geng, D. Wloch, N. Herrera, K. Oksman, Large-scale manufacturing of ultra--strong, strain-responsive poly (lactic acid)-based nanocomposites reinforced with cellulose nanocrystals, Compos. Sci. Technol. 194 (2020) 108144.
[89] L.M. Matuana, S.S. Karkhanis, N.M. Stark, R.C. Sabo, Cellulose nanocrystals as barrier performance enhancer of extrusion-blown PLA films for food applications, Rev. Process (Non-Refereed) (2016).
[90] G.S. Ezat, A.L. Kelly, M. Youseffi, P.D. Coates, Effect of screw configuration on the dispersion and properties of polypropylene/multiwalled carbon nanotube composite, Polym. Compos. 40 (11) (2019) 4196–4204.
[91] H. Patil, R.V. Tiwari, M.A. Repka, Hot-melt extrusion: from theory to application in pharmaceutical formulation, Aaps Pharmscitech 17 (1) (2016) 20–42.
[92] L. Ma, Y. Zhang, Y. Meng, P. Anusonti-Inthra, S. Wang, Preparing cellulose nanocrystal/acrylonitrile-butadiene-styrene nanocomposites using the master–batch method, Carbohydr. Polym. 125 (2015) 352–359.
[93] V. Mano, S. Chimenti, G. Ruggeri, F.V. Pereira, E.L. de Paula, P (CL-b-LLA) diblock copolymers grafting onto cellulosic nanocrystals, Polym. Bull. 74 (9) (2017) 3673–3688.
[94] J. Mao, H. Abushammala, N. Brown, M.-P. Laborie, Comparative assessment of methods for producing cellulose I nanocrystals from cellulosic sources, in: Nanocelluloses: Their Preparation, Properties, and Applications, ACS Publications, 2017, pp. 19–53.
[95] W. Abdallah, M.R. Kamal, Influence of process variables on physical characteristics of spray freeze dried cellulose nanocrystals, Cellulose 25 (10) (2018) 5711–5730.
[96] O. Shoseyov, D. Kam, T.B. Shalom, Z. Shtein, S. Vinkler, Y. Posen, Nanocellulose composite biomaterials in industry and medicine, in: Extracellular Sugar-Based Biopolymers Matrices, Springer, 2019, pp. 693–784.
[97] N. Pal, S. Banerjee, P. Roy, K. Pal, Melt-blending of unmodified and modified cellulose nanocrystals with reduced graphene oxide into PLA matrix for biomedical application, Polym. Adv. Technol. 30 (12) (2019) 3049–3060.
[98] J. Shojaeiarani, D.S. Bajwa, N.M. Stark, Spin-coating: a new approach for improving dispersion of cellulose nanocrystals and mechanical properties of poly (lactic acid) composites, Carbohydr. Polym. 190 (2018) 139–147.
[99] S. Geng, J. Wei, Y. Aitomäki, M. Noël, K. Oksman, Well-dispersed cellulose nanocrystals in hydrophobic polymers by in situ polymerization for synthesizing highly reinforced bio-nanocomposites, Nanoscale 10 (25) (2018) 11797–11807.
[100] M. Boruvka, L. Behalek, P. Lenfeld, C. Ngaowthong, M. Pechociakova, Structure-related properties of bionanocomposites based on poly (lactic acid), cellulose nanocrystals and organic impact modifier, Mater. Technol. 34 (3) (2019) 143–156.
[101] D. Bondeson, K. Oksman, Polylactic acid/cellulose whisker nanocomposites modified by polyvinyl alcohol, Compos. Part A 38 (12) (2007) 2486–2492.
[102] J. Peng, P.J. Walsh, R.C. Sabo, L.-S. Turng, C.M. Clemons, Water-assisted compounding of cellulose nanocrystals into polyamide 6 for use as a nucleating agent for microcellular foaming, Polymer 84 (2016) 158–166.
[103] L. Rueda, et al., Cellulose nanocrystals/polyurethane nanocomposites. Study from the viewpoint of microphase separated structure, Carbohydr. Polym. 92 (1) (2013) 751–757.
[104] I.T. Seoane, P. Cerrutti, A. Vázquez, L.B. Manfredi, V.P. Cyras, Polyhydroxybutyrate-based nanocomposites with cellulose nanocrystals and bacterial cellulose, J. Polym. Environ. 25 (3) (2017) 586–598.
[105] S. Bano, Y.S. Negi, R. Illathvalappil, S. Kurungot, K. Ramya, Studies on nano composites of SPEEK/ethylene glycol/cellulose nanocrystals as promising proton exchange membranes, Electrochim. Acta 293 (2019) 260–272.
[106] L.G. Germiniani, L.C. da Silva, T.S. Plivelic, M.C. Gonçalves, Poly (ϵ-caprolactone)/cellulose nanocrystal nanocomposite mechanical reinforcement and morphology: the role of nanocrystal pre-dispersion, J. Mater. Sci. 54 (1) (2019) 414–426.
[107] A.N. Frone, et al., Thermal and mechanical behavior of biodegradable polyester films containing cellulose nanofibers, J. Therm. Anal. Calorim. 138 (4) (2019) 2387–2398.
[108] W. Yang, et al., Thermomechanical, antioxidant and moisture behaviour of PVA films in presence of citric acid esterified cellulose nanocrystals, Int. J. Biol. Macromol. (2020).
[109] D. Rigotti, et al., Polylactic acid-lauryl functionalized nanocellulose nanocomposites: microstructural, thermo-mechanical and gas transport properties, Express Polym. Lett. 13 (10) (2019).
[110] E. Espino-Pérez, et al., Cellulose nanocrystal surface functionalization for the controlled sorption of water and organic vapours, Cellulose 23 (5) (2016) 2955–2970.
[111] J. Sapkota, J.C. Natterodt, A. Shirole, E.J. Foster, C. Weder, Fabrication and properties of polyethylene/cellulose nanocrystal composites, Macromol. Mater. Eng. 302 (1) (2017) 1600300.
[112] L. Wang, A.W. Roach, D.J. Gardner, Y. Han, Mechanisms contributing to mechanical property changes in composites of polypropylene reinforced with spray-dried cellulose nanofibrils, Cellulose 25 (1) (2018) 439–448.
[113] D. Bagheriasl, F. Safdari, P.J. Carreau, C. Dubois, B. Riedl, Development of cellulose nanocrystal-reinforced polylactide: a comparative study on different preparation methods, Polym. Compos. 40 (S1) (2019) E342–E349.
[114] Y. Peng, D.J. Gardner, Y. Han, Characterization of mechanical and morphological properties of cellulose reinforced polyamide 6 composites, Cellulose 22 (5) (2015) 3199–3215.
[115] V. Khoshkava, H. Ghasemi, M.R. Kamal, Effect of cellulose nanocrystals (CNC) on isothermal crystallization kinetics of polypropylene, Thermochim. Acta 608 (2015) 30–39.

[116] S.A. Kedzior, L. Graham, C. Moorlag, B.M. Dooley, E.D. Cranston, Poly (methyl methacrylate)-grafted cellulose nanocrystals: one-step synthesis, nanocomposite preparation, and characterization, Can. J. Chem. Eng. 94 (5) (2016) 811–822.
[117] J. Zhang, et al., Cellulose nanocrystal driven microphase separated nanocomposites: enhanced mechanical performance and nanostructured morphology, Int. J. Biol. Macromol. 130 (2019) 685–694.
[118] M.P. Arrieta, E. Fortunati, F. Dominici, E. Rayón, J. López, J.M. Kenny, Multifunctional PLA–PHB/cellulose nanocrystal films: processing, structural and thermal properties, Carbohydr. Polym. 107 (2014) 16–24.
[119] Y.D. Li, Q.Q. Fu, M. Wang, J.B. Zeng, Morphology, crystallization and rheological behavior in poly (butylene succinate)/cellulose nanocrystal nanocomposites fabricated by solution coagulation, Carbohydr. Polym. 164 (2017) 75–82.
[120] S. Zarina, I. Ahmad, Biodegradable composite films based on κ-carrageenan reinforced by cellulose nanocrystal from kenaf fibers, BioResources 10 (1) (2015) 256–271.
[121] H.Y. Mi, X. Jing, J. Peng, M.R. Salick, X.F. Peng, L.S. Turng, Poly (ε-caprolactone)(PCL)/cellulose nano-crystal (CNC) nanocomposites and foams, Cellulose 21 (4) (2014) 2727–2741.
[122] H. Sojoudiasli, M.C. Heuzey, P.J. Carreau, Mechanical and morphological properties of cellulose nanocrystal-polypropylene composites, Polym. Compos. 39 (10) (2018) 3605–3617.
[123] L.S.F. Leite, L.C. Battirola, L.C.E. da Silva, M. do C. Goncalves, Morphological investigation of cellulose acetate/cellulose nanocrystal composites obtained by melt extrusion, J. Appl. Polym. Sci. 133 (44) (2016).
[124] S. Tanpichai, K. Oksman, Cross-linked nanocomposite hydrogels based on cellulose nanocrystals and PVA: mechanical properties and creep recovery, Compos. Part A 88 (2016) 226–233.
[125] H. Kargarzadeh, R.M. Sheltami, I. Ahmad, I. Abdullah, A. Dufresne, Cellulose nanocrystal: a promising toughening agent for unsaturated polyester nanocomposite, Polymer 56 (2015) 346–357.
[126] S. Spinella, et al., Polylactide/cellulose nanocrystal nanocomposites: efficient routes for nanofiber modification and effects of nanofiber chemistry on PLA reinforcement, Polymer 65 (2015) 9–17.
[127] P. Dhar, D. Tarafder, A. Kumar, V. Katiyar, Thermally recyclable polylactic acid/cellulose nanocrystal films through reactive extrusion process, Polymer 87 (2016) 268–282.
[128] V.P. Onbattuvelli, R.K. Enneti, J. Simonsen, K.H. Kate, V.K. Balla, S.V. Atre, Structure and thermal stability of cellulose nanocrystal/polysulfone nanocomposites, Mater. Today Commun. 22 (2020) 100797.
[129] X. Feng, Z. Yang, S. Chmely, Q. Wang, S. Wang, Y. Xie, Lignin-coated cellulose nanocrystal filled methacrylate composites prepared via 3D stereolithography printing: mechanical reinforcement and thermal stabilization, Carbohydr. Polym. 169 (2017) 272–281.
[130] M. Mariano, N. El Kissi, A. Dufresne, Cellulose nanocrystal reinforced oxidized natural rubber nanocomposites, Carbohydr. Polym. 137 (2016) 174–183.
[131] J.P. de Oliveira, G.P. Bruni, M.J. Fabra, E. da Rosa Zavareze, A. López-Rubio, M. Martínez-Sanz, Development of food packaging bioactive aerogels through the valorization of Gelidium sesquipedale seaweed, Food Hydrocolloids 89 (2019) 337–350.
[132] Y. Wang, et al., Rheology of the cellulose nanocrystals filled poly (ε-caprolactone) biocomposites, Polymer 140 (2018) 167–178.
[133] Y. Zhang, et al., Poly (lactic acid)/cellulose nanocrystal composites via the pickering emulsion approach: rheological, thermal and mechanical properties, Int. J. Biol. Macromol. 137 (2019) 197–204.
[134] A. Gupta, W. Simmons, G.T. Schueneman, D. Hylton, E.A. Mintz, Rheological and thermo-mechanical properties of poly (lactic acid)/lignin-coated cellulose nanocrystal composites, ACS Sustain. Chem. Eng. 5 (2) (2017) 1711–1720.
[135] J. Shojaeiarani, D.S. Bajwa, N.M. Stark, S.G. Bajwa, Rheological properties of cellulose nanocrystals engineered polylactic acid nanocomposites, Compos. Part B Eng. 161 (2019) 483–489.
[136] M.P. Motloung, V. Ojijo, J. Bandyopadhyay, S.S. Ray, Morphological characteristics and thermal, rheological, and mechanical properties of cellulose nanocrystals-containing biodegradable poly (lactic acid)/poly (ε-caprolactone) blend composites, J. Appl. Polym. Sci. 137 (19) (2020) 48665.
[137] Y. Li, H. He, B. Huang, L. Zhou, P. Yu, Z. Lv, In situ fabrication of cellulose nanocrystal-silica hybrids and its application in UHMWPE: rheological, thermal, and wear resistance properties, Polym. Compos. 39 (S3) (2018) E1701–E1713.
[138] Z. Ying, D. Wu, Z. Wang, W. Xie, Y. Qiu, X. Wei, Rheological and mechanical properties of polylactide nanocomposites reinforced with the cellulose nanofibers with various surface treatments, Cellulose 25 (7) (2018) 3955–3971.
[139] J.M. Wang, S.J. Ding, T.M. Wu, Rheology, crystallization behavior, and mechanical properties of poly (butylene succinate-co-terephthalate)/cellulose nanocrystal composites, Polym. Test. (2020) 106551.
[140] S.S. Karkhanis, N.M. Stark, R.C. Sabo, L.M. Matuana, Water vapor and oxygen barrier properties of extrusion-blown poly (lactic acid)/cellulose nanocrystals nanocomposite films, Compos. Part A 114 (2018) 204–211.
[141] M.Le Gars, L. Douard, N. Belgacem, J. Bras, Cellulose nanocrystals: from classical hydrolysis to the use of deep eutectic solvents, Hydrolysis of Cellulose, IntechOpen, 2019.
[142] E. Espino-Pérez, et al., Designed cellulose nanocrystal surface properties for improving barrier properties in polylactide nanocomposites, Carbohydr. Polym. 183 (2018) 267–277.
[143] E. Fortunati, et al., Nano-biocomposite films with modified cellulose nanocrystals and synthesized silver nanoparticles, Carbohydr. Polym. 101 (2014) 1122–1133.
[144] E.C. Lengowski, E.A.B. Júnior, K.G. Satyanarayana, Nanocellulose-improved food packaging, Adv. Appl. Polysacch. Compos. 73 (2020) 136–183.
[145] Y.W. Chen, H.V. Lee, J.C. Juan, S.M. Phang, Production of new cellulose nanomaterial from red algae marine biomass Gelidium elegans, Carbohydr. Polym. 151 (2016) 1210–1219.
[146] S. Azizi, M.B. Ahmad, N.A. Ibrahim, M.Z. Hussein, F. Namvar, Preparation and properties of poly (vinyl alcohol)/chitosan blend bio-nanocomposites reinforced by cellulose nanocrystals, Chin. J. Polym. Sci. 32 (12) (2014) 1620–1627.
[147] H. Fukuzumi, T. Saito, T. Iwata, Y. Kumamoto, A. Isogai, Transparent and high gas barrier films of cellulose nanofibers prepared by TEMPO-mediated oxidation, Biomacromolecules 10 (1) (2009) 162–165.
[148] L. Atarés, A. Chiralt, Essential oils as additives in biodegradable films and coatings for active food packaging, Trends Food Sci. Technol. 48 (2016) 51–62.
[149] M. Hasan, et al., Micro crystalline bamboo cellulose based seaweed biodegradable composite films for sustainable packaging material, J. Polym. Environ. 27 (7) (2019) 1602–1612.
[150] Y. Wu, et al., Characterization of an antimicrobial poly (lactic acid) film prepared with poly (ε-caprolactone) and thymol for active packaging, Polym. Adv. Technol. 25 (9) (2014) 948–954.
[151] L. Yue, et al., Surface-modified cellulose nanocrystals for biobased epoxy nanocomposites, Polymer 134 (2018) 155–162.
[152] I.F. Pinheiro, et al., Mechanical, rheological and degradation properties of PBAT nanocomposites reinforced by functionalized cellulose nanocrystals, Eur. Polym. J. 97 (2017) 356–365.
[153] A. Butron, O. Llorente, J. Fernandez, E. Meaurio, J.R. Sarasua, Morphology and mechanical properties of poly (ethylene brassylate)/cellulose nanocrystal composites, Carbohydr. Polym. 221 (2019) 137–145.
[154] Y. Shan, C. Li, Y. Wu, Q. Li, J. Liao, Hybrid cellulose nanocrystal/alginate/gelatin scaffold with improved mechanical properties and guided wound healing, RSC Adv. 9 (40) (2019) 22966–22979.
[155] A. Hivechi, S.H. Bahrami, R.A. Siegel, Investigation of morphological, mechanical and biological properties of cellulose nanocrystal reinforced electrospun gelatin nanofibers, Int. J. Biol. Macromol. 124 (2019) 411–417.
[156] A. Kaboorani, N. Auclair, B. Riedl, V. Landry, Mechanical properties of UV-cured cellulose nanocrystal (CNC) nanocomposite coating for wood furniture, Prog. Org. Coat. 104 (2017) 91–96.
[157] M. Yadav, F.-C. Chiu, Cellulose nanocrystals reinforced κ-carrageenan based UV resistant transparent bionanocomposite films for sustainable packaging applications, Carbohydr. Polym. 211 (2019) 181–194.
[158] F. Li, S.Y.H. Abdalkarim, H.-Y. Yu, J. Zhu, Y. Zhou, Y. Guan, Bifunctional reinforcement of green biopolymer packaging nanocomposites with natural cellulose nanocrystal–Rosin hybrids, ACS Appl. Bio Mater. 3 (4) (2020) 1944–1954.
[159] S. Salmieri, et al., Antimicrobial nanocomposite films made of poly (lactic acid)–cellulose nanocrystals (PLA–CNC) in food applications—part B: effect of oregano essential oil release on the inactivation of Listeria monocytogenes in mixed vegetables, Cellulose 21 (6) (2014) 4271–4285.
[160] J.P. de Oliveira, G.P. Bruni, S.L.M. el Halal, F.C. Bertoldi, A.R.G. Dias, E. da Rosa Zavareze, Cellulose nanocrystals from rice and oat husks and their application in aerogels for food packaging, Int. J. Biol. Macromol. 124 (2019) 175–184.
[161] P. Criado, C. Fraschini, S. Salmieri, M. Lacroix, Cellulose nanocrystals (CNCs) loaded alginate films against lipid oxidation of chicken breast, Food Res. Int. 132 (2020) 109110.
[162] P. Criado, C. Fraschini, D. Becher, F.G. Mendonça Pereira, S. Salmieri, M. Lacroix, Modified cellulose nanocrystals (CNCs) loaded in gellan gum matrix enhance the preservation of agaricus bisporus mushrooms, J. Food Process. Preserv. (2020) e14846.
[163] G. Fotie, L. Amoroso, G. Muratore, L. Piergiovanni, Carbon dioxide diffusion at different relative humidity through coating of cellulose nanocrystals for food packaging applications, Food Packag. Shelf Life 18 (2018) 62–70.
[164] D. Enescu, C. Gardrat, H. Cramail, C.Le Coz, G. Sèbe, V. Coma, Bio-inspired films based on chitosan, nanoclays and cellulose nanocrystals: structuring and properties improvement by using water-evaporation-induced self-assembly, Cellulose 26 (4) (2019) 2389–2401.
[165] S. Azizi, R. Mohamad, Mechanical and barrier properties of kappa-carrageenan/cellulose nanocrystals bio-nanocomposite films, in: Proceedings of the IOP Conference Series: Materials Science and Engineering, 368, 2018.
[166] P. Forssell, R. Lahtinen, M. Lahelin, P. Myllärinen, Oxygen permeability of amylose and amylopectin films, Carbohydr. Polym. 47 (2) (2002) 125–129.
[167] E. Fortunati, M. Peltzer, I. Armentano, A. Jiménez, J.M. Kenny, Combined effects of cellulose nanocrystals and silver nanoparticles on the barrier and migration properties of PLA nano-biocomposites, J. Food Eng. 118 (1) (2013) 117–124.
[168] K. Goodarzi, F.J. Shariatzadeh, A. Solouk, S. Akbari, H. Mirzadeh, Injectable drug loaded gelatin based scaffolds as minimally invasive approach for drug delivery system: CNC/PAMAM nanoparticles, Eur. Polym. J. 139 (2020) 109992.
[169] T. Casalini, F. Rossi, S. Lazzari, G. Perale, M. Masi, Mathematical modeling of PLGA microparticles: from polymer degradation to drug release, Mol. Pharm. 11 (11) (2014) 4036–4048.
[170] A.K. Maurya, A. Mishra, N. Mishra, Nanoengineered polymeric biomaterials for drug delivery system, Nanoeng. Biomater. Adv. Drug Delivery 5 (2020) 109.
[171] L. Ning, C. You, Y. Zhang, X. Li, F. Wang, Synthesis and biological evaluation of surface-modified nanocellulose hydrogel loaded with paclitaxel, Life Sci. 241 (2020) 117137.
[172] Y. Chen, et al., Double stimuli-responsive cellulose nanocrystals reinforced electrospun PHBV composites membrane for intelligent drug release, Int. J. Biol. Macromol. (2020).
[173] Y. Guo, et al., Functional mesoporous silica nanoparticles for delivering nimesulide with chiral recognition performance, Microporous Mesoporous Mater. 294 (2020) 109862.

[174] K.M. Rao, A. Kumar, S.S. Han, Poly (acrylamidoglycolic acid) nanocomposite hydrogels reinforced with cellulose nanocrystals for pH-sensitive controlled release of diclofenac sodium, Polym. Test. 64 (2017) 175–182.
[175] M. Ebrahimi, M. Botelho, W. Lu, N. Monmaturapoj, Development of nanocomposite collagen/HA/β-TCP scaffolds with tailored gradient porosity and permeability using vitamin E, J. Biomed. Mater. Res. Part A 108 (12) (2020) 2379–2394.
[176] S.Y. Ooi, I. Ahmad, M.C.I.M. Amin, Cellulose nanocrystals extracted from rice husks as a reinforcing material in gelatin hydrogels for use in controlled drug delivery systems, Ind. Crops Prod. 93 (2016) 227–234.
[177] M.G. Roberts, et al., Functionalization of Cellulose nanocrystals with POEGMA copolymers via copper-catalyzed azide–alkyne cycloaddition for potential drug-delivery applications, Biomacromolecules 21 (6) (2020) 2014–2023.
[178] N. Naseri, A.P. Mathew, L. Girandon, M. Fröhlich, K. Oksman, Porous electrospun nanocomposite mats based on chitosan–cellulose nanocrystals for wound dressing: effect of surface characteristics of nanocrystals, Cellulose 22 (1) (2015) 521–534.
[179] S. Dong, A.A. Hirani, K.R. Colacino, Y.W. Lee, M. Roman, Cytotoxicity and cellular uptake of cellulose nanocrystals, Nano Life 2 (03) (2012) 1241006.
[180] W. Huang, et al., On-demand dissolvable self-healing hydrogel based on carboxymethyl chitosan and cellulose nanocrystal for deep partial thickness burn wound healing, ACS Appl. Mater. Interfaces 10 (48) (2018) 41076–41088.
[181] W.Y. Tong, et al., Antimicrobial wound dressing film utilizing cellulose nanocrystal as drug delivery system for curcumin, Cellulose 25 (1) (2018) 631–638.
[182] J. Szebeni and P. Haima, "Hemocompatibility of medical devices, blood products, nanomedicines and biologicals," TECOmedical Clinical & Technical Review; TECOmedical: Sissach, Switzerland, 2013.
[183] F. Cheng, et al., Preparation and characterization of 2, 2, 6, 6-tetramethylpiperidine-1-oxyl (TEMPO)-oxidized cellulose nanocrystal/alginate biodegradable composite dressing for hemostasis applications, ACS Sustain. Chem. Eng. 5 (5) (2017) 3819–3828.
[184] R.M. Domingues, M.E. Gomes, R.L. Reis, The potential of cellulose nanocrystals in tissue engineering strategies, Biomacromolecules 15 (7) (2014) 2327–2346.
[185] M.S. Enayati, et al., Development of electrospun poly (vinyl alcohol)-based bionanocomposite scaffolds for bone tissue engineering, J. Biomed. Mater. Res. Part A 106 (4) (2018) 1111–1120.
[186] N.T. Lam, R. Chollakup, W. Smitthipong, T. Nimchua, P. Sukyai, Utilizing cellulose from sugarcane bagasse mixed with poly (vinyl alcohol) for tissue engineering scaffold fabrication, Ind. Crops Prod. 100 (2017) 183–197.
[187] L. Qin, H. Gao, S. Xiong, Y. Jia, L. Ren, Preparation of collagen/cellulose nanocrystals composite films and their potential applications in corneal repair, J. Mater. Sci. Mater. Med. 31 (2020) 55.
[188] W. Gao, L. Sun, Z. Zhang, Z. Li, Cellulose nanocrystals reinforced gelatin/bioactive glass nanocomposite scaffolds for potential application in bone regeneration, J. Biomater. Sci. Polym. Ed. 31 (8) (2020) 984–998.
[189] S. Wan, J. Peng, L. Jiang, Q. Cheng, Bioinspired graphene-based nanocomposites and their application in flexible energy devices, Adv. Mater. 28 (36) (2016) 7862–7898.
[190] H.J. Lee, H.S. Lee, J. Seo, Y.H. Kang, W. Kim, T.H.K. Kang, State-of-the-art of cellulose nanocrystals and optimal method for their dispersion for construction-related applications, Appl. Sci. 9 (3) (2019) 426.
[191] L. Hu, et al., Transparent and conductive paper from nanocellulose fibers, Energy Environ. Sci. 6 (2) (2013) 513–518.
[192] Q. Cheng, et al., Construction of transparent cellulose-based nanocomposite papers and potential application in flexible solar cells, ACS Sustain. Chem. Eng 6 (6) (2018) 8040–8047.
[193] X. Wu, Z. Shi, S. Fu, J. Chen, R.M. Berry, K.C. Tam, Strategy for synthesizing porous cellulose nanocrystal supported metal nanocatalysts, ACS Sustain. Chem. Eng. 4 (11) (2016) 5929–5935.
[194] X. Wu, J. Tang, Y. Duan, A. Yu, R.M. Berry, K.C. Tam, Conductive cellulose nanocrystals with high cycling stability for supercapacitor applications, J. Mater. Chem. A 2 (45) (2014) 19268–19274.
[195] K. Ganguly, D.K. Patel, S.D. Dutta, W.C. Shin, K.T. Lim, Stimuli-responsive self-assembly of cellulose nanocrystals (CNCs): structures, functions, and biomedical applications, Int. J. Biol. Macromol. 155 (2020) 456–469.
[196] T.G. Kim, T.G. Park, Surface functionalized electrospun biodegradable nanofibers for immobilization of bioactive molecules, Biotechnol. Prog. 22 (4) (2006) 1108–1113.
[197] Y. Tang, et al., Screen-printed glucose sensors modified with cellulose nanocrystals (CNCs) for cell culture monitoring, Biosensors 10 (9) (2020) 125.
[198] R. Kato, J.H. Lettow, S.N. Patel, S.J. Rowan, Ion-conducting thermoresponsive films based on polymer-grafted cellulose nanocrystals, ACS Appl. Mater. Interfaces 12 (48) (2020) 54083–54093.
[199] X. Sun, P. Tyagi, S. Agate, L. Lucia, M. McCord, L. Pal, Unique thermo-responsivity and tunable optical performance of poly (N-isopropylacrylamide)-cellulose nanocrystal hydrogel films, Carbohydr. Polym. 208 (2019) 495–503.
[200] A.L. Oechsle, L. Lewis, W.Y. Hamad, S.G. Hatzikiriakos, M.J. MacLachlan, CO_2-switchable cellulose nanocrystal hydrogels, Chem. Mater. 30 (2) (2018) 376–385.
[201] R. Cha, Z. He, Y. Ni, Preparation and characterization of thermal/pH-sensitive hydrogel from carboxylated nanocrystalline cellulose, Carbohydr. Polym. 88 (2) (2012) 713–718.
[202] Y. Tao, S. Liu, Y. Zhang, Z. Chi, J. Xu, A pH-responsive polymer based on dynamic imine bonds as a drug delivery material with pseudo target release behavior, Polym. Chem. 9 (7) (2018) 878–884.
[203] J. Shojaeiarani, D. Bajwa, A. Shirzadifar, A review on cellulose nanocrystals as promising biocompounds for the synthesis of nanocomposite hydrogels, Carbohydr. Polym. 216 (2019) 247–259.